BBA - Bioenergetics 1859 (2018) 1025–1038

Contents lists available at ScienceDirect

BBA - Bioenergetics

journal homepage: www.elsevier.com/locate/bbabio

In pea stipules a functional photosynthetic electron flow occurs despite a reduced dynamicity of LHCII association with photosystems

Martina Giovanardi[a,1], Laura Pantaleoni[a,1], Lorenzo Ferroni[a,1], Cristina Pagliano[b], Pascal Albanese[b], Costanza Baldisserotto[a], Simonetta Pancaldi[a,*]

[a] Laboratory of Plant Cytophysiology, Department of Life Sciences and Biotechnology, Università degli Studi di Ferrara, Corso Ercole I 'd'Este 32, 44121 Ferrara, Italy
[b] Applied Science and Technology Department - BioSolar Lab, Politecnico di Torino, Environment Park, Via Livorno 60, 10144 Torino, Italy

ARTICLE INFO

Keywords:
Chlorophyll fluorescence
Native gel electrophoresis
Phosphorylation
Photosystem
Pisum sativum
Thylakoid membrane

ABSTRACT

The flexible association of the light harvesting complex II (LHCII) to photosystem (PS) I and PSII to balance their excitation is a major short-term acclimation process of the thylakoid membrane, together with the thermal dissipation of excess absorbed energy, reflected in non-photochemical quenching of chlorophyll fluorescence (NPQ). In *Pisum sativum*, the leaf includes two main photosynthetic parts, the basal stipules and the leaflets. Since the stipules are less efficient in carbon fixation than leaflets, the adjustments of the thylakoid system, which safeguard the photosynthetic membrane against photodamage, were analysed. As compared to leaflets, the stipules experienced a decay in PSII photochemical activity. The supramolecular organization of photosystems in stipules showed a more conspicuous accumulation of large PSII-LHCII supercomplexes in the grana, but also a tendency to retain the PSI-LHCI-LHCII state transition complex and the PSI-LHCI-PSII-LHCII megacomplexes probably located at the interface between appressed and stroma-exposed membranes. As a consequence, stipules had a lower capacity to perform state transitions and the overall thylakoid architecture was less structurally flexible and ordered than in leaflets. Yet, stipules proved to be quite efficient in regulating the redox state of the electron transport chain and more capable of inducing NPQ than leaflets. It is proposed that, in spite of a relatively static thylakoid arrangement, LHCII interaction with both photosystems in megacomplexes can contribute to a regulated electron flow.

1. Introduction

In higher plants and green algae the light-driven reactions of oxygenic photosynthesis are coordinated by four multi-subunit protein complexes embedded in the thylakoid membrane that include Photosystems (PS) II and I, their light harvesting complexes (LHC) II and I, Cytochrome (Cyt) b_6f complex and ATP synthase (ATPase). The two PSs are connected through plastoquinone (PQ) pool, Cyt b_6f complex and plastocyanin, working in series to transform light energy into chemical energy. Among all the complexes involved in photosynthesis, PSII is the major target of acclimation (see e.g. [1]). PSII is a water-plastoquinone oxidoreductase complex, because its activity is to initiate the photosynthetic electron transfer chain by using light as a driving force and water as the electron source [2]. The PSII reaction centre is composed of the integral proteins D1 and D2 - which bind most of the redox cofactors of the electron transport chain inside PSII -, the intrinsic light-harvesting proteins, CP43 and CP47 - which bind the majority of the chlorophyll *a* (Chl *a*) molecules of PSII -, and the α and β subunits of cytochrome *b*559 (Cyt*b*559). The complex comprising the reaction centre, several low molecular mass integral subunits and the three extrinsic polypeptides forming the oxygen evolving complex is called PSII core, which is now well-established to occur in a functional dimeric form (C_2) [3–5]. Most of the Chls, and especially the major part of Chl *b*, are located in the peripheral LHCII. Major antenna of PSII is a trimeric LHCII composed of a combination of the *Lhcb1–3* gene products. Minor LHCII are instead monomers and are the products of *Lhcb4*, *Lhcb5* and *Lhcb6* genes, which originate Lhcb4 (CP29), Lhcb5 (CP26) and Lhcb6 (CP24) proteins, respectively. LHCII trimers can bind the PSII core strongly (S), at CP43 side through CP26, or with moderate (M) affinity, at CP47 side through CP24 and CP29, to form PSII-LHCII supercomplexes with different orders of association, which varies from C_2S up to the largest $C_2S_2M_2$ supercomplex [5–11] and even bigger megacomplexes [12,13].

At the ultrastructural level, inside the chloroplast, the thylakoid

* Corresponding author.
E-mail address: simonetta.pancaldi@unife.it (S. Pancaldi).
[1] These authors contributed equally to the study.

https://doi.org/10.1016/j.bbabio.2018.05.013
Received 16 January 2018; Received in revised form 17 May 2018; Accepted 23 May 2018
Available online 24 May 2018

system is differentiated into stroma lamellae and appressed membranes of grana stacks. A peculiar characteristic of thylakoid membranes is that PSII-LHCII supercomplexes form densely packed macrodomains located in the grana stacks, ensuring efficient light absorption and energy transfer, whereas PSI and ATPase are mainly located at the grana margins and stroma lamellae [8,14,15]. Cyt b_6f localization is more controversial and probably depends on the width regulation of the stromal gap between adjacent membranes of the grana stacks [16]. The structure of the thylakoid membrane is not rigid and the organization of protein complexes in the membranes undergoes dynamic variations responding to changes in the environmental conditions [17–19]. These can occur on a long time scale (weeks, months, seasons), as long-term responses, or in the range of seconds to minutes, involving short-term re-arrangements [1,8,20–24]. Long-term acclimation strategies occur to optimize photosynthetic efficiency under stable light gradients. One of the main acclimation responses to light is the adjustment of PSII/PSI reaction centre stoichiometry [8,20,22,25], as well as of LHCII/photosystems stoichiometry, with a consequent re-modulation of the chloroplast ultrastructure, in particular grana stacking, number of grana per chloroplast, and thylakoid lumen width [20,21,26]. The amount of the other photosynthetic proteins is also modified to support maximal rates of photosynthesis related to the light intensity [20,27]. Conversely, short-term responses to varying light conditions involve thylakoid architectural changes without biosynthesis or degradation of photosynthetic proteins [28,29]. The capacity of ATP and NADPH consumption in the Calvin-Benson cycle is the ultimate reason driving changes in thylakoid structure, which in turn reflects the adjustments necessary to ensure a fluent electron transport chain from PSII to final acceptors (e.g., [25]). However, the main task for plants on a short-time scale is not principally to maximize photosynthesis, but rather to avoid photodamage. Non-photochemical quenching (NPQ) mechanisms and state transitions are considered the major short-term acclimation processes. NPQ reflects the thermal dissipation of excess energy induced by the acidification of the thylakoid lumen. Many research efforts have been spent to elucidate NPQ induction, including the role of the PsbS protein, the involvement of the xanthophyll cycle pigments and lutein, and the structural re-arrangements of antenna complexes which can be permissive to the quenched state (e.g., [30–33]). State transitions promote the redistribution of the absorbed light energy between the two photosystems by means of a reversible association of a fraction of mobile LHCII trimers to PSI or PSII (reviewed in [34]). During “state 2”, typically induced by red light that preferentially excites PSII, but also triggered by low light, the phosphorylation of LHCII is induced by reduced PQ pool and LHCII is found associated to PSI, to form the so-called “state-transition complex” PSI-LHCI-LHCII; conversely, “state 1” is promoted by far-red light, which preferentially excites PSI, but it is also found in darkness and under high light conditions, and is induced by dephosphorylation of LHCII trimers and their association to PSII [19,35,36]. In the past, several studies on thylakoid membranes and their rearrangement during state transition processes proposed an important role of M trimers to detach from $C_2S_2M_2$ supercomplexes and associate to PSI forming the PSI-LHCI-LHCII complex in “state 2” [37,38]. However, more recent findings have instead investigated the role of a fraction of LHCII trimers called “extra LHCII pool” that should be involved in state-transition processes upon short-term acclimation, maintaining the absorption balance between the two photosystems [22,24,39]. According to these theories, the mobile LHCII fraction should not be part of the PSII-LHCII supercomplexes embedded in the inner grana discs, but it is rather located in the grana margins, where it is ready to associate to PSI in the stroma-exposed regions under “state 2” [40]. Consequently, PSII-LHCII supercomplexes located in the appressed grana regions should not be influenced in their organization and assembly by state transition phenomena [23,40]. Based on several lines of evidence, state transitions have recently been re-interpreted as a regulatory mechanism involving extensive PSI-LHCI-PSII-LHCII interactions, giving rise to large megacomplexes at the grana margins, which can fine-tune energy balance between photosystems under natural fluctuations of white light [41–43]. At present, research on the organization flexibility of large megacomplexes is considered of utmost importance to understand plant survival on land [44].

Although the thylakoid membrane of higher plants is one of the best-characterized biomembranes, many aspects are still controversial especially about its dynamics [28]. In this concern, important advancement in the understanding of PSII-LHCII supercomplexes has been achieved in recent years using thylakoids isolated from *Pisum sativum* (pea) leaves [11,12,17,45–48]. Nevertheless, the use of pea as a model for studies of the photosynthetic membrane should take into consideration that a pea leaf is morphologically heterogeneous, because it includes two main photosynthetic parts, i.e., the basal stipules and the lamina divided into leaflets. This may have no significant impact, as several reports have documented the high relevance of stipules to the overall pea leaf photosynthesis [49–52]. However, in our laboratories, preliminary investigations (see Results Section 3.1) actually revealed that the carbon fixation capacity of pea stipules is consistently lower than in leaflets. The different photosynthetic performance of pea stipules and leaflets prompted us to compare the thylakoid organization in their chloroplasts.

2. Material and methods

2.1. Plant material, growth conditions and light treatments

Seeds of *Pisum sativum* L. var. Paladio were germinated on filter paper moistened with tap water at 20 °C. After germination, seedlings were planted into plastic flower pots (three plants in each flower pot, 10 cm of diameter) and transferred inside a Cr60 Secret Jardin indoor growing box equipped with white LEDs with photon flux density of 100 $\mu mol_{photons}\, m^{-2}\, s^{-1}$, photoperiod of 8:16 h light:darkness and temperature of 26 °C [46]. Plants were daily watered before the beginning of the dark period. For analyses, first expanded leaflets and stipules were harvested from different plants of at least three weeks. Pigment content analysis, gas exchange measurements and fluorescence analyses were obtained from plants sampled around the middle of photoperiod (i.e., ca. 4 h after the onset of light). For the biochemical and ultrastructural analyses, leaves were sampled under three different conditions: (a) dark-acclimated leaves, at the end of the night period; (b) leaves treated for 15 min with 25 $\mu mol_{photons}\, m^{-2}\, s^{-1}$ far red light (FR) at the end of the night period; (c) growth-light-exposed leaves (GL), sampled at the steady state in the middle of photoperiod.

2.2. Photosynthetic pigment extraction and quantification

Photosynthetic pigments were extracted from pre-weighted small round pieces of leaflets and stipules with a surface area of 28.27 mm^2. Extraction was performed with 100% methanol for 10 min at 80 °C and pigment concentration was determined according to Wellburn [53] using a Pharmacia Ultrospec 2000 UV–Vis spectrophotometer (1 nm bandwidth) (Amersham Biosciences, Piscataway, NJ, USA). Pigments were quantified both on surface area unit and on fresh weight unit basis. At least four replicates were analysed for both leaflets and stipules.

2.3. CO_2 gas exchange

CO_2 gas exchange was determined using an LCA-4 type open system infrared gas analyzer (ADC BioScientific Ltd., Hoddesdon, UK). Analyses were performed in vivo placing inside the measuring chamber unexcised leaflets or stipules. At least four replicates were analysed for each leaf portion. The difference in the CO_2 flow entering and exiting the measuring chamber was monitored for 7 min. Firstly, dark respiration values were determined measuring the CO_2 concentration in darkness. Subsequently, increasing light intensities from 25 to 1800 $\mu mol_{photons}\, m^{-2}\, s^{-1}$ were

applied for net photosynthesis determination. Light was provided by 4 LED mono 3000 K CRI70LXR7-SW30 (Philips). Samples were incubated for stabilisation for 4 min inside the measuring chamber before the determination of CO_2 values at every change of light intensity. After the measurements, the surface area of analysed leaflets and stipules was determined using ImageJ free software (National Institutes of Health, Bethesda, MD, USA). Gas exchange was determined both on surface unit and on chlorophyll unit basis. Light saturated rate of photosynthesis (PhN_{max}), apparent quantum yield (k) and photosynthetic light compensation point (LCP) were calculated according to Peek et al. [54] with OriginPro 2015 program (OriginLab Corp., Northampton, MA, USA) using the model equation $PhN = PhN_{max}\ [1 - e^{-k(I-LCP)}]$, were I refers to irradiance.

2.4. Modulated chlorophyll fluorescence

Pulse amplitude modulated fluorescence traces were recorded with a Junior-PAM chlorophyll fluorimeter (Heinz Walz, Effeltrich, Germany). To obtain light curves, small pieces of leaflets and stipules were maintained on wet filter paper and pre-incubated in darkness for 30 min. Basal fluorescence values F_0 was determined and maximum fluorescence F_M was measured flashing the samples with a saturating light pulse. Maximum PSII quantum yield was determined as $F_V/F_M = (F_M - F_0)/F_M$. Samples were subsequently exposed to a sequence of increasing actinic light intensities from 25 to 1500 $\mu mol_{photons}\, m^{-2}\, s^{-1}$ (blue LED with emission at 450 nm, focussed on the sample through fiber optics). Each exposure lasted 7 min. At the end of each period, steady-state fluorescence F_t and maximum fluorescence value F_M' were determined. At least six biological replicates were analysed for both leaflets and stipules. The fluorescence values were combined using the set of equations proposed by Hendrickson et al. [55]. The formalism based on the model is that of quantum yields for the partitioning of the energy absorbed by PSII among processes in competition (see [56]). The correctness of the energy partitioning model has been recently questioned [57], but the use of such parameters remains highly informative of the photosynthetic physiology. In particular, $Y(PSII) = (F_M' - F_t)/F_M'$ is the quantum yield of PSII photochemistry; $Y(NO) = F_t/F_M$ is related to non-regulatory energy loss and is an excellent tool to highlight defects in the regulation of the plastoquinone redox state [58,59]; $Y(NPQ) = F_t/F_M' - F_t/F_M$ is related to regulatory photoprotective energy dissipation, i.e. exciton life time in the antenna reflected by NPQ [56].

For state transition measurements, samples were prepared and pre-incubated in darkness for F_M determination. Subsequently a light treatment protocol was applied to promote contrasting fluorescence states, as described by Lokstein et al. [60], Wientjes et al. [24] and Ferroni et al. [61]. In particular, samples were illuminated with far red light (provided by LED with 730 nm emission wavelength) for 10 min, followed by 15 min exposure to actinic light (25 $\mu mol_{photons}\, m^{-2}\, s^{-1}$ provided by LED with 450 emission wavelength) and finally by 25 min exposure to combined actinic and far red light. F_M' values were determined every minute applying a saturating pulse. F_M' measured after 15 min exposure to actinic light (F_{M2}), which reflects the maximum State 2, and F_M' measured at the end of the experiment (F_{M1}), when State 1 was induced, were used to calculate the qT parameter $[qT = (F_{M1} - F_{M2})/F_{M1}]$, according to Wientjes et al. [24].

2.5. Thylakoid isolation

Thylakoid membranes were isolated according to Järvi et al. [62] from leaflets and stipules of 3–4 plant sets that were treated as described in Section 2.1. All buffers were supplemented with 10 mM NaF to inhibit the phosphatases. Thylakoids were rapidly frozen and stored in liquid nitrogen. Chl content of thylakoid membranes was determined by extraction with 80% (v/v) acetone [53].

2.6. SDS-PAGE and immunoblotting

Thylakoid proteins were separated by SDS-PAGE according to Laemmli [63] on a 15% acrylamide resolving gel containing 6 M urea. For the subsequent detection of proteins, 0.5, 1.0, and 2.0 μg of Chl of each thylakoid sample were loaded on each gel. After electrophoresis, proteins were visualised by Coomassie staining overnight followed by destaining for 5 h, or blotted onto a nitrocellulose membrane (Schleicher and Schuell, Dessel, Germany). Western blotting was performed with standard techniques, in particular membranes were blocked in TBS buffer (10 mM Tris-HCl pH 7.4 and 1.5 M NaCl) supplemented with 0.5% Bovine Serum Albumine. Immunodetection was performed with protein-specific antibodies: ATP-β subunit of ATPase, PsaA subunit of PSI, CP43 and D1 subunits of PSII, Lhcb1 and Lhcb6 subunit of LHCII and Cyt f subunit of Cyt b_6f (Agrisera codes: AS05085, AS06172, AS111787, AS05084, AS01004, AS01010, AS08306 respectively).

Thylakoid phosphoproteins were detected with an antibody against phosphothreonine (P-Thr) (Cell Signalling Technology, code 9381). Goat anti-rabbit secondary antibody in conjunction with alkaline phosphatase (Agrisera, code AS06607) was used for protein detection. To avoid any deviation between different immunoblots, thylakoids from leaflets and stipules of each light condition were loaded onto the same gel and antibody dilution was checked in the linearity range. The optimal antibody dilution was checked in the linearity range for all the phosphorylated proteins at the same time intentionally, in order to compare their phosphorylation level simultaneously. Densitometry measurements of phosphoprotein band signals were performed with the GelDoc XR + imager (Bio-Rad), by using Quantity One software version 4.6.9 (Bio-Rad). Quantitative comparison was performed on the basis of the slope value of the line interpolating the three incremental values of intensity for each condition tested [17].

2.7. Native PAGE and second dimension (2D) electrophoresis

Thylakoids (8 μg Chl) were solubilized in darkness on ice for 2 min with dodecyl β-D-maltoside (β-DM; Sigma) at a final concentration of 1.5% (w/v), followed by centrifugation at 18,000g at 4 °C for 15 min, or with digitonin (Calbiochem) at a final concentration of 2% (w/v) at room temperature for 10 min under gentle agitation, followed by centrifugation at 18,000g for 20 min [64]. Thylakoid complexes solubilized with β-DM were analysed by blue-native (BN) PAGE, while those solubilized with digitonin were separated by large-pore blue-native (lpBN) PAGE, according to the protocols described by Järvi et al. [62]. Native electrophoresis was performed with an Emperor Penquin™ Dual Gel Electrophoresis System (Owl Separation Systems, Portsmouth, The Netherlands) at 0 °C for 3.5 h by gradually increasing the voltage from 75 to 200 V. Quantification of band volume was performed with ImageJ software and quantitative comparison of bands was performed applying two-factor ANOVA [64]. After native-PAGE, the lanes were cut out and incubated in Laemmli buffer [63] containing 10% (w/v) SDS and 5% (v/v) β-mercaptoethanol for 1 h, followed by separation of the protein subunits of the complexes in the second dimension (2D) with SDS-PAGE (12% polyacrylamide and 6 M urea). After electrophoresis, proteins were visualised by silver staining.

2.8. Microscopy

Small round pieces (28.27 mm^2) were collected from different leaf portions of several plants exposed to the light treatments as explained in Section 2.1. Samples were prepared for transmission electron microscopy as described in Baldisserotto et al. [65]. Semithin sections of the samples were stained with toluidine blue and observed under a Zeiss Axiophot light microscope. Ultrathin sections were instead observed with a Hitachi H800 transmission electron microscope (TEM) (Electron Microscopy Centre, Ferrara University, Italy). For morphometric analyses, granum thickness, number

of thylakoids per granum and thylakoid thickness were measured in chloroplasts from different micrographs; in particular, grana stacks were chosen in the central region of the organelle and only those sectioned almost perpendicularly to the membrane plane were used for measurements. The number of grana analysed with the software ImageJ was in the range of 26–54 per type of sample.

2.9. Statistical analyses

Data were statistically treated using Student's *t*-test for comparison of means of two data sets or one-factor analysis of variance (ANOVA) for analysis of multiple data sets; two-factor ANOVA was used to separate the effect of two sources of variation (leaf part; light treatments). In each case, ANOVA was followed by Tukey's *post hoc*. Threshold for statistical significance was set at $P < 0.05$. Elaboration was performed with Origin2018 (OriginLab Corp., Northampton, MA, USA).

3. Results

3.1. Photosynthetic energy conversion is lower in stipules than in leaflets

3.1.1. Leaf tissue organization, pigment content and carbon fixation

The semithin cross section of leaflets and stipules was analysed under the light microscope. A typical organization of a low-light acclimated plant was observed for leaflets, with one palisade layer and a spongy layer rich of air spaces (Fig. 1A). Stipules appeared with a less structured tissue organization, i.e. with a palisade layer composed by roundish cells and a more compact spongy mesophyll layer as compared to leaflets. Stipule cross-sections were 10% thinner than leaflets (0.167 ± 0.022 mm of stipules vs 0.185 ± 0.021 mm of leaflets, $P < 0.001$). To avoid discrepancies linked to the different thickness of the photosynthetic leaf portions, the pigment content was normalized on the basis of a fresh weight unit (Table 1). Pigments were extracted with methanol, one of the fastest and most effective solvents for rapid Chl screening. However, because of its acidic character, it leads to some degree of Chl allomerization and, therefore, underestimates Chl *a*/*b* ratio [66]. Nevertheless, methanolic extracts still provided a good estimation of total pigment content, revealing no difference in Chls and carotenoids between leaflets and stipules (Table 1). Total Chl content was used for subsequent analysis of carbon fixation rates on the basis of a Chl unit (Fig. 1B). The two photosynthetic leaf portions markedly differed in CO_2 gas exchange in darkness, as well as at very low light. Indeed, stipules showed extremely higher respiration rate in darkness (+180%, $P < 0.05$; Fig. 1C) and light compensation point (55 $\mu mol_{photons}\, m^{-2}\, s^{-1}$ vs 24 $\mu mol_{photons}\, m^{-2}\, s^{-1}$ in leaflets, +130%, $P < 0.05$) than leaflets (Fig. 1D). Interestingly stipules maintained a consistently lower PhN than leaflets. However, supported by the same apparent quantum yield of CO_2 fixation, the difference in PhN was non-significant between leaflets and stipules when they reached their maximum PhN (Fig. 1E, F).

3.1.2. PSII activity and thermal dissipation

Fluorescence was measured after exposure of several replicates of leaflets and stipules to a sequence of increasing light intensities. The

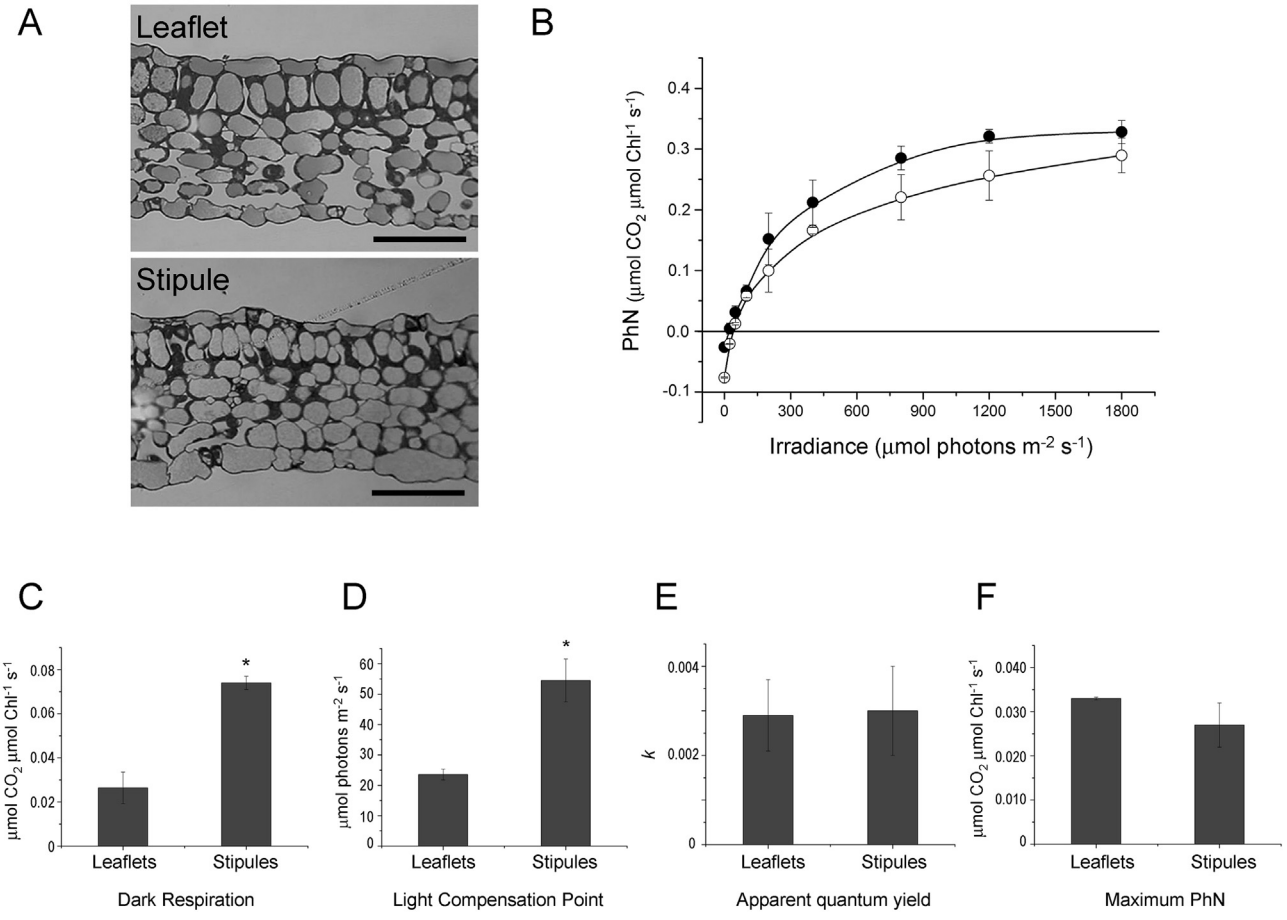

Fig. 1. Cross section morphology and CO_2 gas exchange in leaflets and stipules of *Pisum sativum*.
(A) Representative cross sections of a leaflet and a stipule. Bars: 100 µm. (B) Net photosynthesis rate (PhN) calculated per Chl unit in leaflets (filled circles) and stipules (empty circles) upon increasing light intensity. (C) Dark respiration. (D) Light compensation point. (E) Maximum net photosynthesis. (F) Apparent quantum yield of CO_2 fixation. Data are averages of at least $N = 4$ replicates ± standard deviation. *: $P < 0.05$ according to Student's *t*-test for statistical comparison of data.

Table 1
Pigment composition, Chl *a*/*b* and Chl/carotenoids ratios in leaflets and stipules of *P. sativum*. Values are expressed in mg g^{-1} of fresh weight. Data are replicates of at least $N = 4$ samples and are expressed as average ± standard deviation. No significant differences were found based on Student's *t*-test at $P < 0.05$.

	Chl *a*	Chl *b*	Carotenoids	Chl *a*/*b*	Chl/carotenoids
Leaflets	1.10 ± 0.19	0.54 ± 0.10	0.15 ± 0.02	2.02 ± 0.10	11.09 ± 0.66
Stipules	0.94 ± 0.28	0.49 ± 0.14	0.12 ± 0.04	1.91 ± 0.10	11.63 ± 0.93

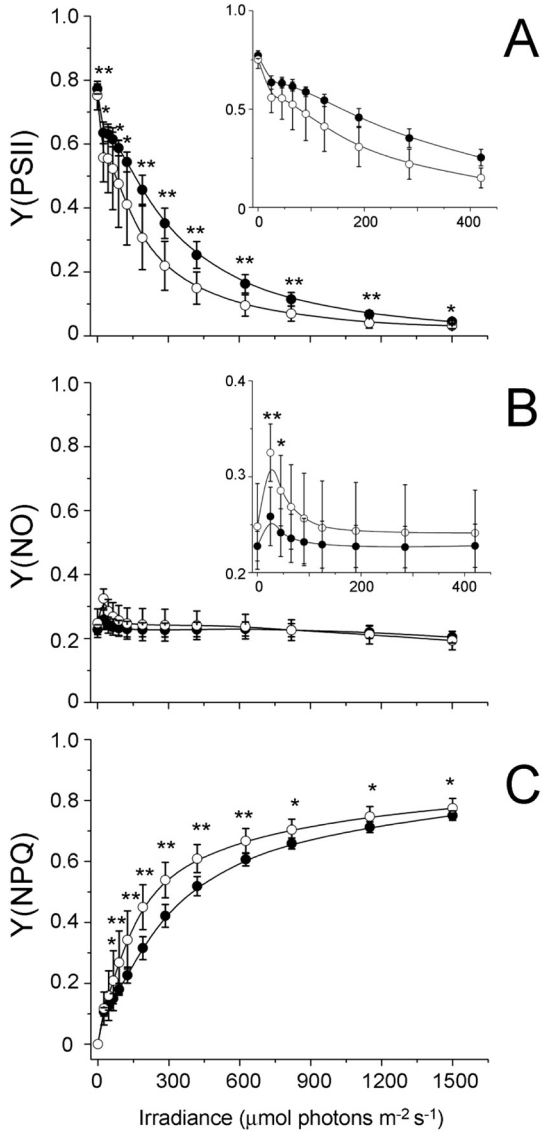

Fig. 2. Light curves of PAM fluorescence yields in leaflets (filled circles) and stipules (empty circles) of *Pisum sativum*.
(A) Quantum yield of PSII photochemistry Y(PSII). In the insert curves are compared in the low-medium irradiance range; (B) Yield of the constitutive energy loss Y(NO). In the insert, curves are compared in the low-medium irradiance range. The irradiances resulting in significantly different Y(NO) are shown in the insert; (C) Yield of regulatory thermal dissipation Y(NPQ). Values are average of at least $N = 6$ replicates ± standard deviation. *: $P < 0.05$, **: $P < 0.01$ according to Student's *t*-test for statistical comparison of data.

fluorescence parameters recorded during the measuring routine were combined to calculate three quantum yields (Fig. 2). The actual yield of PSII [Y(PSII)] is the energy fraction used for PSII photochemistry. After dark incubation, the maximum Y(PSII), F_V/F_M, was 0.77 in leaflets, a value in line with those reported in plants grown under low-light regimes [67]. In stipules, F_V/F_M was slightly, but significantly, lower (0.72, $P < 0.01$; Fig. 2A). Y(PSII), as expected, decreased upon increasing light intensities in both leaf portions. However, Y(PSII) was consistently lower in stipules than in leaflets. At 25 and 50 $\mu mol_{photons}\, m^{-2}\, s^{-1}$, the lower Y(PSII) was compensated by a peak of Y(NO) (Fig. 2B, insert). According to its original interpretation [55], Y(NO) represents the energy fraction passively dissipated as heat or fluorescence. More recently, it has been used as a parameter to monitor the redox state of the PQ at the PSII acceptor side [58,59,68]. The peak in Y(NO) found at low irradiance revealed indeed a more reduced state of PQ pool in stipules as compared to leaflets. However, at higher light intensities, the photosynthetic electron flow was enough fluid in stipules to restore Y(NO) values overlapping with those of leaflets. At irradiances higher than 65 $\mu mol_{photons}\, m^{-2}\, s^{-1}$, the lower Y(PSII) was compensated by a higher Y(NPQ) (Fig. 2C). Y(NPQ) is related to the thermal dissipation of excess energy by light-dependent regulatory mechanisms. Therefore, at irradiances higher than 65 $\mu mol_{photons}\, m^{-2}\, s^{-1}$ the lower capability to use the absorbed light energy for PSII photochemistry in stipules took advantage of a higher capacity of thermal dissipation.

3.2. *In stipules larger PSII-LHCII supercomplexes are preferentially accumulated*

Based on functional analyses, the lower photosynthetic capacity of stipules could affect PSII organization, because it seemed that PSII was more exposed to excitation energy pressure than in leaflets. Therefore, we investigated the general thylakoid composition and, in particular, the supramolecular organization of PSII in grana stacks.

The key proteins belonging to major thylakoid complexes PsaA of PSI, ATPβ of ATPase, CP43 and D1 of PSII, Cyt *f* of Cyt b_6f complex, Lhcb1 subunit of the major LHCII, and Lhcb6 of the minor LHCII were detected by immunoblot analyses of thylakoids isolated from leaflets and stipules. As shown in Fig. 3, no differences were found between leaflets and stipules, except for an evidently enhanced signal of Lhcb6 (about twofold, $P < 0.01$, Student's *t*-test, $N = 3$).

Since no relevant difference was found for PSII and major LHCII amounts, BN-PAGE was performed using β-DM to solubilize the entire thylakoid membranes and compare the supramolecular organization of PSII between leaflets and stipules. Taking into account the different photosynthetic efficiency of leaflets and stipules especially under low light and the contentious involvement of granal PSII-LHCII supercomplexes in short-term responses to low light [24,37,40], the dynamicity of thylakoid membranes was tested comparing plants previously exposed to different light conditions: i) after the daily dark phase, when "State 1" was expected; ii) after the daily dark phase and subsequent incubation with FR light for 15 min, in order to trigger maximum "State 1" and iii) under growth-light (GL) conditions (100 $\mu mol_{photons}\, m^{-2}\, s^{-1}$) at the steady state in the middle of photoperiod, to induce "State 2". After BN-PAGE (Fig. 4), the thylakoid protein-complexes separated on 2D SDS-PAGE maps (Fig. 5) revealed a pattern similar to several previous reports in model angiosperm *Arabidopsis thaliana* [6,69,70] and confirmed also in pea leaf [17]. In particular, in the uppermost part of the gels four types of PSII-LHCII supercomplexes were resolved, in addition to larger megacomplexes (Fig. 5A). In particular, the four bands were assigned to the well-known supercomplexes formed by a PSII core dimer associated with increasing amounts of trimeric LHCII: C_2S, C_2S_2, C_2S_2M, $C_2S_2M_2$ (Fig. 5A, B). The volume of each band corresponding to PSII-LHCII supercomplexes was evaluated and, in order to eliminate potential effects due to unequal gel loadings, for each lane the volumes were normalized to that of the most intense band, containing almost all thylakoid PSI-LHCI, together with

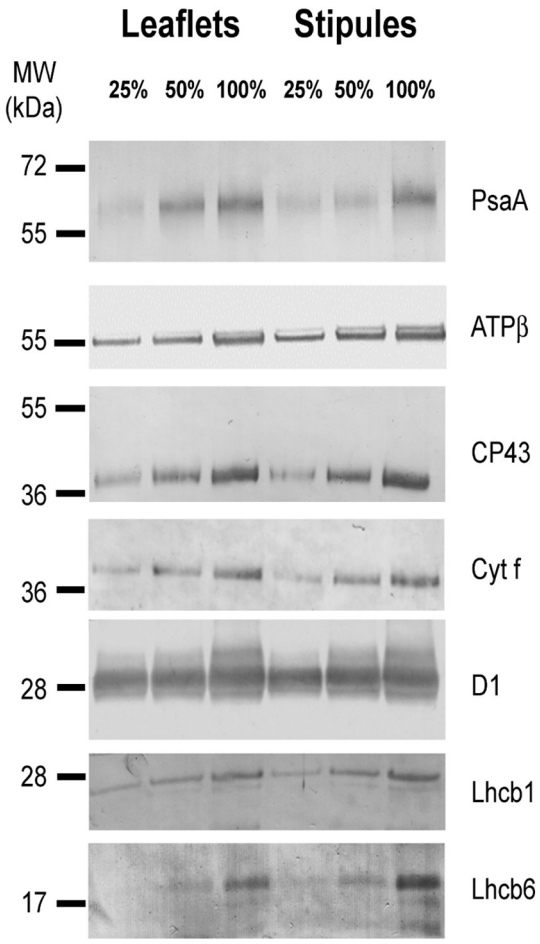

Fig. 3. Immunodetection of subunits representative for the main thylakoid protein complexes in *Pisum sativum* leaflets and stipules.
Thylakoid proteins were separated by SDS-PAGE and subsequently blotted onto a nitrocellulose membrane for immunodetection of PsaA subunit of PSI, ATPβ subunit of ATPase, CP43 subunit of PSII, Cyt *f* subunit of Cyt b_6f, D1 subunit of PSII, Lhcb1 subunit of major LHCII and Lhcb6 of minor LHCII. At 100% of band intensity, 2 μg of Chl were loaded on gels. Molecular weight marker is indicated on the left, and corresponds to a Fermentas PageRuler™ Prestained Protein Ladder Plus (#SM1819). Representative membranes are shown.

nearly co-migrating PSII dimer and ATPase (Fig. 5B). A two-factor ANOVA was then used to separate the effects of two variables *LS* (leaflet vs. stipule) and *light* (dark, FR, GL treatments), as well as to test their interaction [64]. The *light* variable did not have any significant effect on the pattern of supercomplexes (Fig. 5C). Conversely, *LS* variable had a significant impact: as compared to leaflets, stipules were enriched in the largest PSII-LHCII supercomplexes C_2S_2M and $C_2S_2M_2$, while they had a lower proportion of C_2S_2 (Fig. 5C). Interaction between the two variables was not significant for any PSII-LHCII supercomplexes. Finally, 2D maps as in Fig. 5B suggested that stipules contained more megacomplexes than leaflets (Fig. 5B).

3.3. LHCII pool is less dynamic in stipules than in leaflets

While analysis of native complexes after β-DM solubilization revealed a clear difference between stipules and leaflets with respect to the organization of PSII-LHCII supercomplexes, it did not help understand potential differences in the dynamics of the whole antenna system.

3.3.1. Ability to perform state transitions

The ability of leaflets and stipules to perform state transitions was evaluated through short-term light treatments, which promote preferential excitation of PSII (induction of “State 1”) or PSI (induction of “State 2”) (Fig. 6A). After dark-acclimation, irradiation with only FR caused an increase in F_M'/F_M in leaflets and suggested that a partial association of the LHCII pool to PSI occurred in darkness and could be reversed by a preferential excitation of PSI with FR, leading to an increase in PSII fluorescence. This occurred instead very marginally in stipules.

Subsequently, LHCII was induced to serve PSI (“State 2”) treating the leaf portions with a blue actinic light of low intensity (AL, 25 $\mu mol_{photons}\, m^{-2}\, s^{-1}$) for several minutes. As shown in Fig. 6A, the F_M'/F_M value expectedly lowered in leaflets, whereas it remained significantly higher in stipules ($P < 0.05$ during all the 25-min AL exposure).

Finally, the combination of FR and AL until the end of the experiment was used to trigger again a “State 1” condition in order to compare the extent of the state transition. The reversible antenna relocation from PSI to PSII is in fact responsible for relatively small changes in F_M' reflecting variations in PSII absorption cross section [23,60]. In leaflets the increase in F_M'/F_M ratio occurred quite promptly and was evident; conversely, recovery of fluorescence was slower and less marked in stipules (Fig. 6A). State transitions were quantified in relative terms, as FR-reversible F_M' as compared to F_M' in state I, according to the qT analysis reported by Wientjes et al. [23]. In stipules, ability to perform state transitions was 35% lower than in leaflets (Fig. 6B).

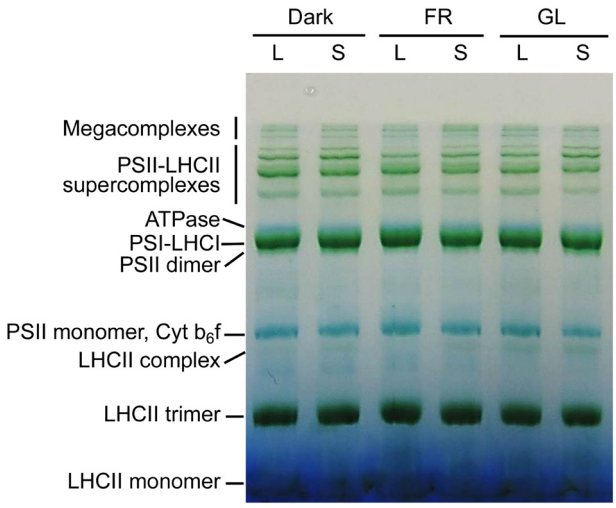

Fig. 4. BN-PAGE of thylakoid protein complexes from leaflets (L) and stipules (S) of *Pisum sativum* extracted after the daily dark phase (dark), far-red light treatment (FR) or during growth-light incubation at the steady state (GL).
Thylakoids were solubilized with 1.5% β-DM, 8 μg Chl were loaded on gel for each sample. Attribution of bands to specific complexes was based on 2D BN/SDS-PAGE separation, as exemplified in Fig. 5B.

3.3.2. Dynamic phosphorylation of LHCII and PSII

To support the results of the biophysical analyses and verify the occurrence of the state-transition process, the phosphorylation level of the main thylakoid proteins was analysed by the P-Thr antibody on Western blots of thylakoid membranes isolated from plants treated as described in methods Section 2.1 and in results Section 3.2 (Fig. 7A). In dark-acclimated plants, the phosphorylation level of Lhcb1 and Lhcb2 proteins of major LHCII (hereafter referred to as LHCII) was found 3.5 times higher in stipules than in leaflets (Fig. 7B). Upon exposure to FR light, which should promote the maximum “State 1” condition, this difference was even higher, further confirming the hypothesis that LHCII pool was less dynamic in stipules, with a tendency to remain in a phosphorylated state (Fig. 7B). Finally, when plants were exposed to GL, the phosphorylation of LHCII did not differ between leaflets and

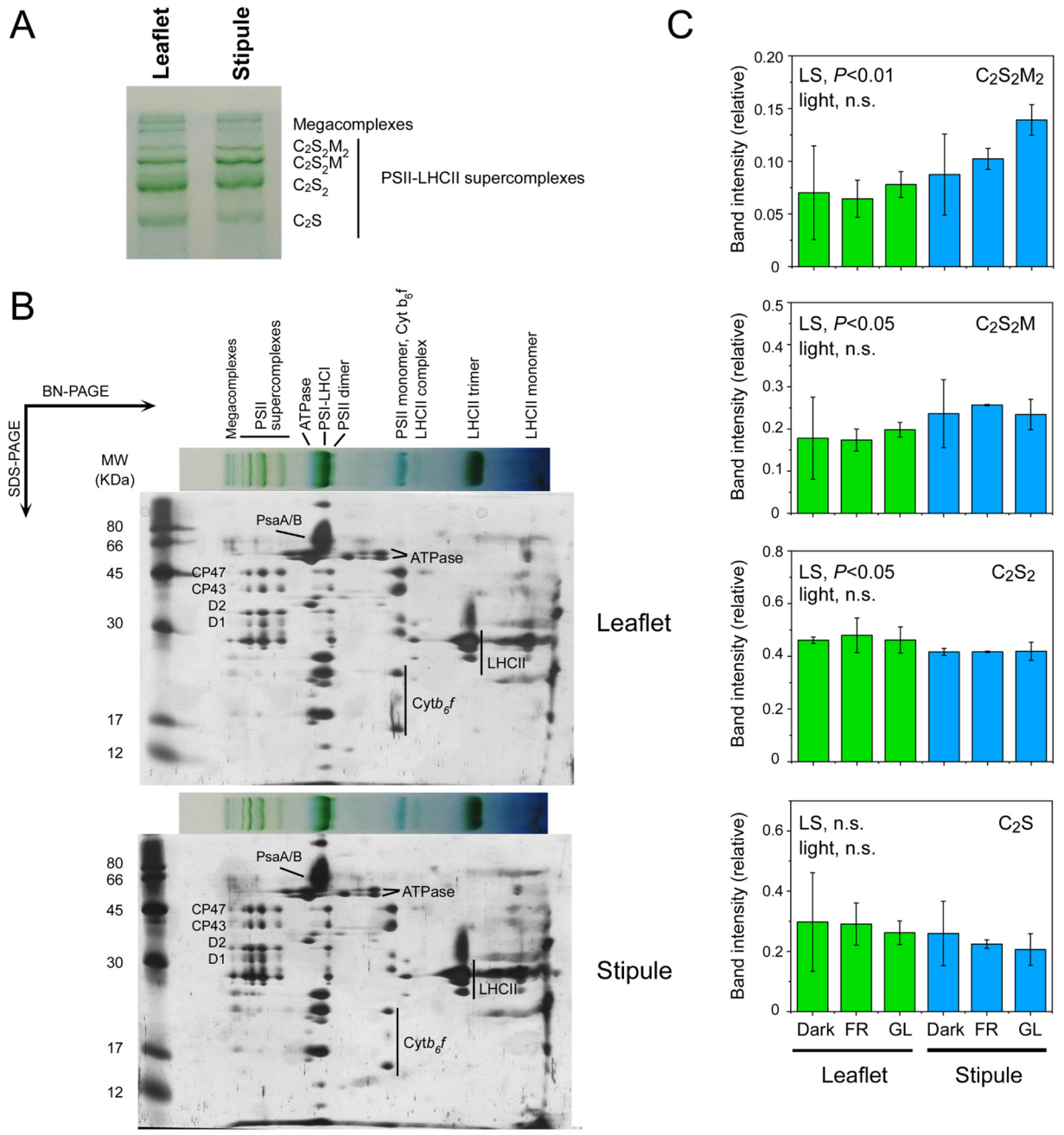

Fig. 5. Analysis of PSII-LHCII supercomplexes separated through BN-PAGE of thylakoids isolated from leaflets and stipules of *Pisum sativum* and solubilized with β-DM.

(A) Detail of the uppermost portion of the BN-PAGE gel shown in Fig. 4 (GL samples). Four types of supercomplexes are indicated and named according to Albanese et al. [17] in *P. sativum* leaves. (B) Bidimensional SDS-PAGE of thylakoid protein complexes. The highlighted silver-stained spots correspond to CP47, CP43, D2 and D1 subunits of PSII, some Cyt b_6f subunits, PsaA/B subunits of PSI, two subunits of ATPase, and the main subunits of the major LHCII. Marker molecular weight of proteins is reported on the left. (C) Densitometric quantification of PSII-LHCII supercomplexes separated by BN-PAGE. Band volumes were quantified in gels as in Fig. 4 and normalized to the most intense band (PSI-LHCI) for each lane. Data were analysed with a two-factor ANOVA to separate the effect of two variables and their interaction: *LS*, leaflet vs. stipule; *light*, light treatments (dark, dark-acclimated condition; FR, far red incubation; GL, growth light-acclimated condition). Each graph reports average ± standard deviation of three-four replicates, as well as the influence of the two variables with the corresponding probability (threshold at $P < 0.05$; n.s., non-significant effect). Interaction between *LS* and *light* variables was not significant in each case.

stipules (Fig. 7B). Conversely, the PSII reaction centre proteins (i.e., CP43, D2 and D1) showed a negligible phosphorylation level in dark-acclimated plants (Fig. 7A) and, upon exposure to FR and GL, presented a similar trend of phosphorylation in stipules and in leaflets (Fig. 7A).

3.3.3. Complexes residing in non-appressed thylakoid domains

Analysis of qT and thylakoid protein phosphorylation was strongly indicative of a less flexible interaction of LHCII with PSI in stipules. Such labile interactions can be demonstrated solubilizing the thylakoids with the very mild detergent digitonin [62]. Incapability of digitonin to penetrate the grana appressions excludes the granal PSII-LHCII supercomplexes from solubilization.

The lpBN-PAGE profiles of the thylakoid-protein complexes solubilized with digitonin were compared between leaflets and stipules exposed to the same short-term light treatments used for the phosphorylation analysis (Fig. 8A). Identity of native bands was assessed by 2D

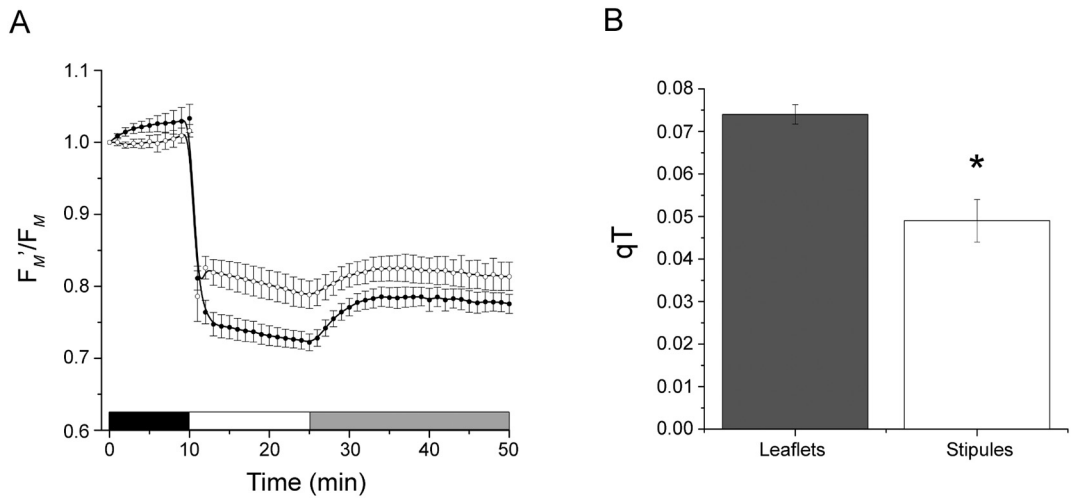

Fig. 6. Evaluation of state transitions in leaflets and stipules of *Pisum sativum*.
(A) Time-course of F_M'/F_M ratio in leaflets (closed circles) and stipules (open circles) during 10 min of far-red light (black bar), 15 min of actinic light (white bar) and 25 min of combined far red and actinic blue light (grey bar). (B) qT values in leaflets and stipules. In both cases, values are averages ± standard deviation of 7–8 replicates. *: $P < 0.05$ according with Student's *t*-test for statistical comparison of data.

SDS-PAGE gels and a representative map corresponding to leaflets under steady-state GL is reported in Fig. 8B. The thylakoid protein complexes pattern was compared with those reported for the model angiosperm *Arabidopsis thaliana* [40,62,71]. The nomenclature of megacomplexes is that reported in Suorsa et al. [40]. From higher to lower molecular weight, mc1, the first megacomplex of high abundance and just entering the running gel, comprised a large amount of PSI-LHCI subunits as well as of LHCII. In the following megacomplex, with slightly lower molecular weight than mc1 and not well resolved in the first dimension, also PSII subunits were present, thus corresponding to a large PSI-LHCI-PSII-LHCII megacomplex, here indicated as mc(I–II). After that, a series of megacomplexes, not clearly resolved, contained PSI, LHCI and LHCII subunits. The megacomplex mc5 was the following clearly resolved and contained PSI, PSII, LHCI and LHCII subunits. The mc5 results from the co-migration of PSI-LHCI-LHCII with a certain amount of $C_2S_2M_2$, i.e. a few granal PSII-LHCII supercomplexes that reside closer to grana margins and can be solubilized by digitonin [72]. Slightly lower, the so-called mc6 and mc8 were both composed of only PSI-LHCI. The state-transition-specific complex, PSI-LHCI-LHCII, was then identified and was composed of PSI, LHCI and LHCII subunits, but not of PSII. Subsequently, a very intense band contained a large amount of PSI, almost co-migrating with ATPase subunits, followed by a slightly faster migrating very small amount of PSII dimer. The subsequent bands were identified as: PSII in the monomeric form; Cyt b_6f co-migrating with LHCII assembly complex; free trimers of LHCII and, finally, LHCII monomers (Fig. 8B).

Short-term light treatments are known to modify the pattern of complexes residing in the non-appressed thylakoid regions [40]. From lpBN-PAGE (Fig. 8A), it was evident that the main band exhibiting large variability was that of the PSI-LHCI-LHCII state-transition complex. To enhance band visualization in the region of the largest complexes, lpBN-PAGE was silver stained (Fig. 9A). Variations were indeed not limited to the state-transition complex, but involved likewise the megacomplexes, in a way determined by both the leaf part analysed (variable *LS*) and the light treatment (variable *light*). In order to dissect specific effects of either variables, band volumes were determined. In particular, the following band(s) were analysed: mc1, neatly resolved at the top of lpBN gels; mc(I–II), as the density migrating slightly faster than mc1; mc5, mc6, mc8, analysed together as PSI-LHCI-LHCII non-state transition megacomplexes; PSI-LHCI-LHCII state-transition complex. Band volumes were then normalized to the volume of the major band, corresponding to PSI-LHCI and ATPase. This normalization compensated for different degrees of thylakoid solubilization with digitonin. Moreover, because the ATPase is not directly involved in dynamic changes of thylakoid complexes, the normalization was also informative about the distribution of PSI-LHCI among different complexes including or not LHCII. The normalized band volumes were analysed with two-factor ANOVA and results are reported in Fig. 9B. We found that the two variables, *LS* and *light*, had independent effects on specific megacomplexes, without any statistically significant interaction. As already evident from a visual analysis of lpBN profiles (Fig. 8A), the amount of state-transition complex was highly dynamic in response to the *light* variable. In both leaflets and stipules, GL and FR conditions resulted in two contrasting effects; in particular, under FR the state-transition complex tended to disappear. In dark-acclimated samples, an intermediate pattern between FR and GL samples was found. Interestingly, the *LS* variable had a significant impact as well; in fact, the relative amount of state-transition complex was consistently more represented in stipules than in leaflets (see especially the very similar values obtained in dark-acclimated stipules and GL-exposed leaflets, Fig. 9B). The mc1 showed a pattern of light-dependent variation roughly similar to that of the state-transition complex, but no changes were dependent on *LS*. Conversely, the other complexes formed by PSI-LHCI and LHCII (mc5, mc6, mc8) did not show any significant change in their collective amount. Quite singular was instead the dynamics of mc(I–II). Two-factor ANOVA pointed to a significant effect of the *light* variable, but also suggested some effect due to *LS* variable, yielding a *P* value just above the 0.05 threshold. A global data analysis with one-factor ANOVA and *post hoc* Tukey's test indicated that the relative amount of mc(I–II) in FR-exposed stipules was indeed significantly higher than in the other samples. Therefore, thylakoids of stipules revealed a specific tendency to host not only higher amounts of state-transition complexes, but also more extensive PSI-LHCI-LHCII-PSII interactions in mc(I–II) under a condition of oxidized electron transport chain (Fig. 9B).

3.4. Typical short-term dynamic changes in thylakoid architecture occur in leaflets, but not in stipules

The flexible LHCII association with photosystems is a main determinant for thylakoid re-arrangements and, indeed, the chloroplast ultrastructure has been shown to respond to changes in light quality within a time scale of minutes [73]. Given the considerably reduced LHCII dynamism observed in stipules, we used transmission electron

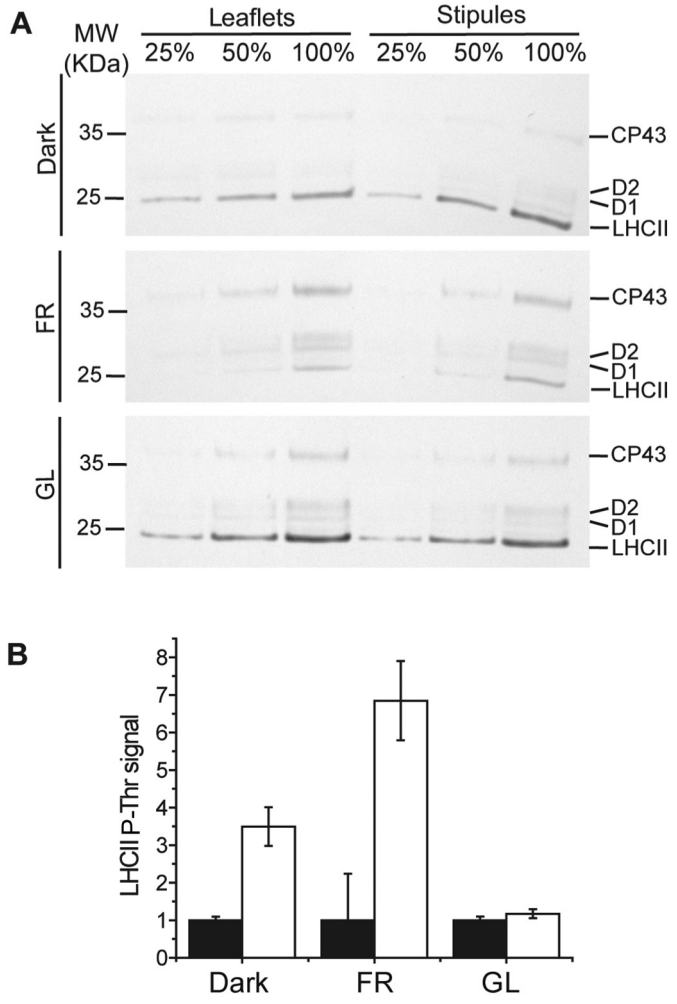

Fig. 7. Phosphorylation levels of thylakoid proteins in leaflets and stipules of *Pisum sativum* after exposure to the daily dark phase (dark), far-red light treatment (FR) and growth light at the steady state (GL).
(A) Examples of Western blotting membranes used for the quantification showing a linear increase in the P-Thr specific antibody signal. At 100%, 2 μg of Chl were loaded. (B) Relative quantification of P-Thr signals of LHCII in stipules (white bar) as compared to leaflets (black bar) after dark exposure (dark), far-red light treatment (FR) and growth light exposure at the steady state (GL). Values are average ± standard deviation of three replicates. Data were normalized to the P-Thr signal in leaflets.

microscopy to evaluate whether it had an impact on the thylakoid architecture in comparison with leaflets. As for previous analyses, plants were exposed to different light treatments promoting the mechanism of state transition. Representative micrographs are shown in Fig. 10.

The chloroplasts of the dark-acclimated leaflets contained a well-ordered thylakoid system, with grana stacks and stroma lamellae in general arranged regularly along the main axis of the organelle (Fig. 10A). An apparent increase in thylakoid stacking under FR caused a somewhat less ordered arrangement of thylakoids (Fig. 10C). The thylakoid system appeared quite regularly organized also under GL conditions, when the enlargement of the thylakoid lumen and the accumulation of some starch granules were evident (Fig. 10E).

In stipules, in general the thylakoid system appeared less ordered under each condition in comparison with the leaflet counterpart. This was evident in the dark-acclimated chloroplasts, in which groups of thylakoid lamellae and grana appeared separated by large, clear stroma regions (Fig. 10B). Different from leaflets, TEM images from FR-exposed stipules did not evidence an increase in grana stacking, rather showed some thylakoid swelling (Fig. 10D). Finally, in the GL-acclimated stipules the thylakoid system appeared even more disordered, mainly because the extent of thylakoid swelling was very inhomogeneous even within a single granum (Fig. 10F). In fact, the lumen enlargement was much more conspicuous in the granal end-membrane thylakoids, as if the granum stack had a limited capacity to flexibly support the light-induced accumulation of protons in the lumen. No starch grains were observed in these chloroplasts (Fig. 10F).

On the right of each chloroplast image of Fig. 10, a detail of the thylakoid stacking of the corresponding type of sample is shown. Morphometric data of grana are reported in Table 2. Dark-adapted leaflets showed the minimum average granum thickness, mainly linked to a low thylakoid thickness as compared to GL samples. In fact, the same average number of thylakoids per granum was found in dark- and light-acclimated leaflets. On the opposite, FR-treated leaflets showed the same granum thickness of light-acclimated leaflets, but also the same thylakoid lumen vertical expansion of dark-adapted leaflets, thus resulting in a much higher number of thylakoids per granum, i.e., a higher stacking degree. Finally, in leaflets the transition from dark to growth light promoted the expansion of the thylakoid lumen, indicative of an active accumulation of protons in lumen during the light-driven photosynthetic reactions.

It is interesting to note that in stipules the transition from dark to GL, as well as the treatment with FR light, did not induce marked variations in average granum thickness, thylakoid thickness and number of thylakoids per granum, which always resembled those of light-adapted leaflets.

4. Discussion

There can be many explanations for a leaf, or a leaf part, to yield a low photosynthetic capacity. One of these can be a high respiration rate, which is indeed one main reason for pea stipules to be less efficient in CO_2 fixation than leaflets (Fig. 1C). PhN is lower in stipules because they require more light to balance respiration (i.e., they have higher light compensation point LCP, Fig. 1D). However, at higher irradiance, stipules are still less efficient photosynthetic performers than leaflets (Fig. 1B), suggesting other profound physiological differences between the two leaf parts, including constraints due to anatomical features, e.g. leading to gas diffusional limitations in more compact stipule mesophyll (Fig. 1A; see [74]) or also limitations in sugar exportation to sinks (see [75]). Independent of the causes, stipules experience a tighter bottleneck in energy flow from the light harvesting to utilization for carbon fixation. Occurrence of a limitation in the capacity to consume reducing equivalents produced by the light reactions is demonstrated by the lower Y(PSII) in comparison with leaflets (Fig. 2A). Y(PSII) is found lower than in leaflets over the entire range of steady-state irradiances, suggesting that stipules are more prone to PSII photoinhibition (Fig. 2A). The lower F_V/F_M of stipules could be evidence that the risk is actual. However, comparison of Y(NO) between leaflets and stipules suggests that a fluent electron flow is still permitted in stipules. Y(NO) can be used as a simple index of the reduction state of the PQ pool, especially to highlight significant de-regulations of the electron transport chain impacting on photosystem integrity [58,68]. A well-regulated electron transport chain tends to keep Y(NO) at low values [58,59,76]. In stipules, some increase in Y(NO) occurs only at irradiance lower than LCP (Figs. 1 and 2B), but when approaching the irradiance of growth, Y(NO) already overlaps with that of leaflets, helped by the induction of the thermal dissipation through *NPQ*, evidently more active in stipules (Fig. 2C).

An element ensuring an efficient management of the absorbed light energy in stipules is indeed their higher capacity to induce *NPQ* as compared to leaflets (Fig. 2C). This higher capacity for *NPQ* is strongly suggestive of an active cyclic electron flow around PSI [77,78], which is again consistent with a low capacity of NADPH use in the Calvin-Benson cycle. This inference introduces another intriguing aspect of the energy management in stipules, regarding the energy distribution

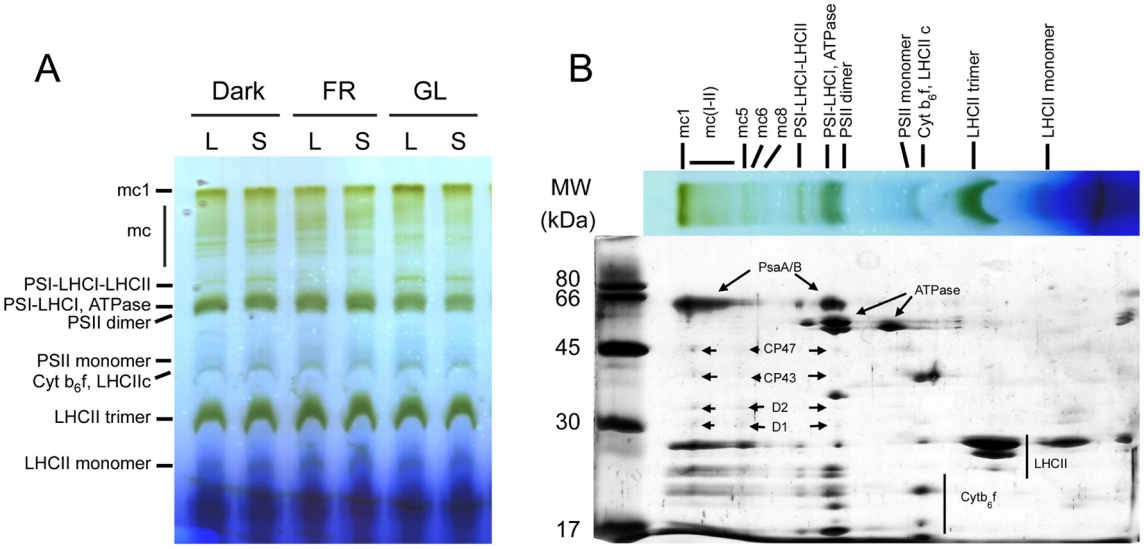

Fig. 8. Thylakoid complexes residing in non-appressed thylakoid domains, as revealed by lpBN-PAGE of thylakoids isolated from *Pisum sativum* leaflets (L) and stipules (S) and solubilized with digitonin. (A) lpBN-PAGE of thylakoid protein complexes isolated after the daily dark phase (dark), far-red light treatment (FR) or after growth light incubation at the steady state (GL). Thylakoids were solubilized with 2% digitonin, 8 μg Chl were loaded on each lane. (B) 2D SDS-PAGE of thylakoid protein complexes of leaflets maintained in growth light before thylakoid extraction (GL). The highlighted silver-stained spots correspond to CP47, CP43, D2 and D1 subunits of PSII core, PsaA/B subunits of PSI, ATPase subunits, major LHCII subunits and Cytb_6f subunits. Marker molecular weight of proteins is reported on the left. Nomenclature of resolved complexes is according to Suorsa et al. [40]; mc(I–II), megacomplexes including PSI-LHCI and PSII-LHCII; LHCIIc, LHCII assembly complex.

between PSI and PSII allowed by LHCII. In higher plants, the model of state-transition-like processes has been progressively refined up to recent years (among others, [34,35,43,79]). In both pea leaflets and stipules, negligible changes in the pattern of granal PSII-LHCII supercomplexes upon different light treatments indicate that the mobile LHCII is not, or not mainly, recruited from PSII-LHCII supercomplexes (see [37]), but instead corresponds to the “extra LHCII” pool [24,39–41]. In leaflets, the flexible association of LHCII to PSII or PSI through state-transition-like processes matches expectations: under growth light, a population of LHCII, upon STN7 kinase-mediated phosphorylation induced by reduced PQ, is found associated with PSI in the state-transition complex PSI-LHCI-LHCII (Figs. 7, 9; [36,80]). As a dynamic regulation in the short term, the process is promptly reversible when the PQ is oxidized in darkness and even more when the leaflet is exposed to FR light, leading to dephosphorylation of LHCII and disassembly of PSI-LHCI-LHCII (Figs. 7, 9). Different from leaflets, in stipules, the lpBN-PAGE profiles, the LHCII phosphorylation levels and the fluorescence dynamics, all depict a substantial reduction in the dynamism of non-appressed thylakoid regions in response to changes in light quantity and quality [20,40,81]. Quite stable association of LHCII with PSI can have a positive impact to support the cyclic electron flow around PSI [34], which probably self-sustains an efficient system of electron recycling to the PQ pool. As a result, reduced PQ in turn promotes LHCII phosphorylation and association to PSI even in darkness, while protons pumped in the thylakoid lumen allow an effective *NPQ* induction as soon as light exceeds the LCP (Figs. 1D, 2C; [77,82,83]). However, the behaviour of stipules is problematic when the electron outflow through PSI is stimulated by FR light.

Both in leaflets and stipules, exposure to FR light results in the disassembly of most state-transition complexes as compared to the corresponding GL condition (Fig. 9B), but nonetheless the capacity for qT is smaller in stipules (Fig. 6). This result cannot be satisfactorily explained by traditional models of energy balance between photosystems through state transitions mediated by mobile LHCII [35]. According to Grieco et al. [41], not only the state-transition complex, but also the extensive LHCII connectivity in the megacomplexes controls the energy distribution between PSI and PSII at the grana margins. Some of these megacomplexes, which we indicate as mc(I–II), include both PSI and PSII and are presumably located at the interface of grana and stroma thylakoids, where PSI and PSII can interact through a loosely bound population of LHCII, so that the function of the two photosystems can be dynamically balanced, allowing a fluent linear electron flow [41,72] and other regulatory processes of energy distribution between the photosystems, in particular a photoprotective energy spillover from PSII to PSI [44,64,84,85]. In leaflets, the amount of mc(I–II) relative to “free PSI-LHCI” does not undergo any relevant variation under FR, GL or dark incubation (Fig. 9B). This suggests that the modulation of the energy transfer properties of the LHCII lake bridging PSI and PSII could not require an extensive mobility of LHCII, but rather be fine-tuned by the phosphorylation of LHCII [41,86]. Certainly more challenging is the response of mc(I–II) in stipules exposed to FR light (Fig. 9B). What is clear is that mc(I–II) is largely retained in FR-treated stipules, apparently because of a low sensitivity of PSI-LHCI-PSII-LHCII interactions to an oxidized PQ pool and possibly supported by higher levels of LHCII phosphorylation (Fig. 6B). Noticeably, in stipules the detection of a significant band of PSI-PSII megacomplexes even after β-DM solubilization (Fig. 5B) suggests that some additional structural factors presumably limit the mobility of thylakoid complexes [87]. Therefore, the association of PSI-LHCI with PSII-LHCII is a constant property of the stipule thylakoid membrane – with an important impact on the overall architecture of the thylakoid system.

The thylakoid system of leaflet chloroplasts repeats well-known changes in organization upon short-term light treatments [20,73,87], i.e., thylakoid ultrastructure is fully representative of the biochemical flexibility in photosynthetic complexes association. The thylakoid system of stipule chloroplasts, although in some aspects similar to that of leaflets under GL, appears instead affected by a certain degree of disorder, only partially relieved by the FR treatment (Fig. 10A vs. B, E vs. F). The organization of PSII-LHCII supercomplexes in the appressed membranes, in particular the protein crowding and their ordered/scattered arrangement, are key determinants of the thylakoid structure [28]. Moreover, pairs of the large C_2S_2M supercomplexes can interact vertically and possibly further stabilize the contact of adjacent thylakoids in grana [45]. Interestingly, comparing pea and bean leaves, Rumak et al. [48] concluded that the higher density of PSII-LHCII

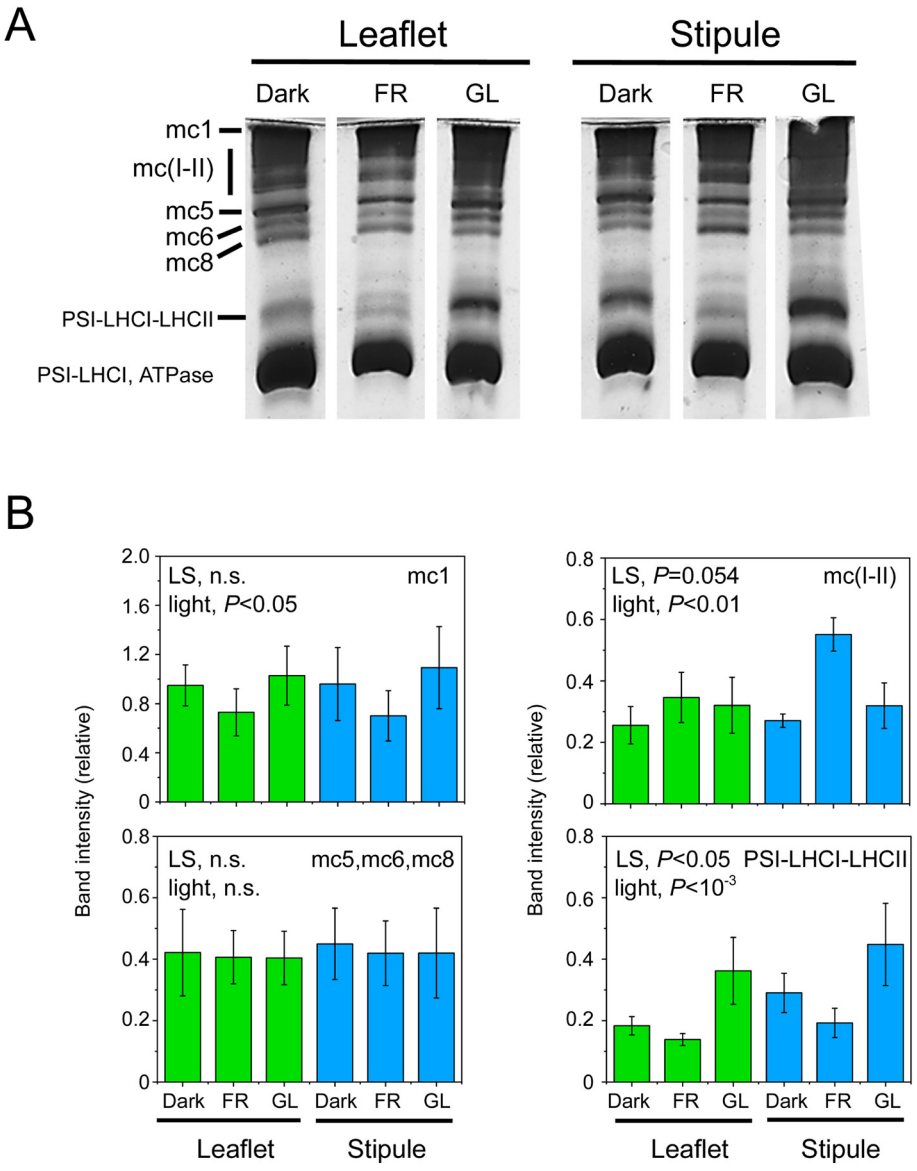

Fig. 9. Large thylakoid complexes revealed by lpBN-PAGE of thylakoids isolated from *Pisum sativum* leaflets and stipules and solubilized with digitonin as in Fig. 8A.

(A) Detail of the uppermost portion of an lpBN-PAGE gel as shown in Fig. 8A after silver staining to enhance band contrast. Lanes have been re-ordered for easier comparison of samples within each leaf portion. Nomenclature as in Fig. 8B. (B) Densitometric quantification of the large complexes separated by lpBN-PAGE. Band volumes were quantified in gels as in Fig. 8A and normalized to the most intense band containing PSI-LHCI and ATPase for each lane. Data were analysed with a two-factor ANOVA to separate the effect of two variables and their interaction: *LS*, leaflet vs stipule; *light*, light treatments (dark, dark-acclimated condition; FR, far red incubation; GL, growth light-acclimated condition). Each graph reports average ± standard deviation of three-four replicates, as well as the influence of the two variables with the corresponding probability (threshold at $P < 0.05$; n.s., non-significant effect). Interaction between *LS* and *light* variables was not statistically significant in each case.

supercomplexes in grana thylakoids of bean resulted in a quite unordered thylakoid arrangement as compared to pea. Very likely in pea stipules a higher density of large supercomplexes can similarly contribute to the less ordered appearance of the entire system. In fact, a characterizing aspect of stipules thylakoids is a higher tendency to accumulate $C_2S_2M_{(2)}$ supercomplexes (Fig. 5C), whose organization depends on the availability of the linking monomeric antennae Lhcb4 and Lhcb6 that mediate the connection of M-LHCII trimers to C_2S_2 [5]. Therefore, one structural ground for stipules to accumulate more $C_2S_2M_{(2)}$ is a higher amount of Lhcb6 (Fig. 3). Together with granal PSII-LHCII supercomplexes, the presence of PSI-LHCI-(PSII)-LHCII megacomplexes very likely residing at the grana margins represents another important mechanical constraint against a modulable arrangement of the thylakoid system in stipules (see also [88]). The consequence is apparent especially in the grana of stipules exposed to GL. In stipules the osmotic enlargement of the thylakoid lumen caused by the influx of ions is probably limited because of a more rigid organization of the megacomplexes, so that thylakoid swelling is allowed only in the end-membrane thylakoids facing the stroma (Fig. 10F). A hindered swelling of inner thylakoids in the stack can restrict the access of lumenal proteases involved in D1 degradation [89], thus probably co-operating to the accumulation of PSII-LHCII supercomplexes in stipules.

The development of large, green stipules represents an investment in photosynthetic components for a pea plant, and this presupposes a return in terms of photosynthetic capacity [75]. Stipules have a thylakoid membrane in which the well-known structural flexibility, believed a necessary requisite for functionality, is substantially down-regulated, because of extensive association of LHCII to PSII in appressed domains and of more stable association of LHCII with both PSI and PSII in grana margins. Nevertheless, the intersystem LHCII connectivity [41] probably still endows photosystems with the flexibility which safeguards the integrity of the photosystems themselves.

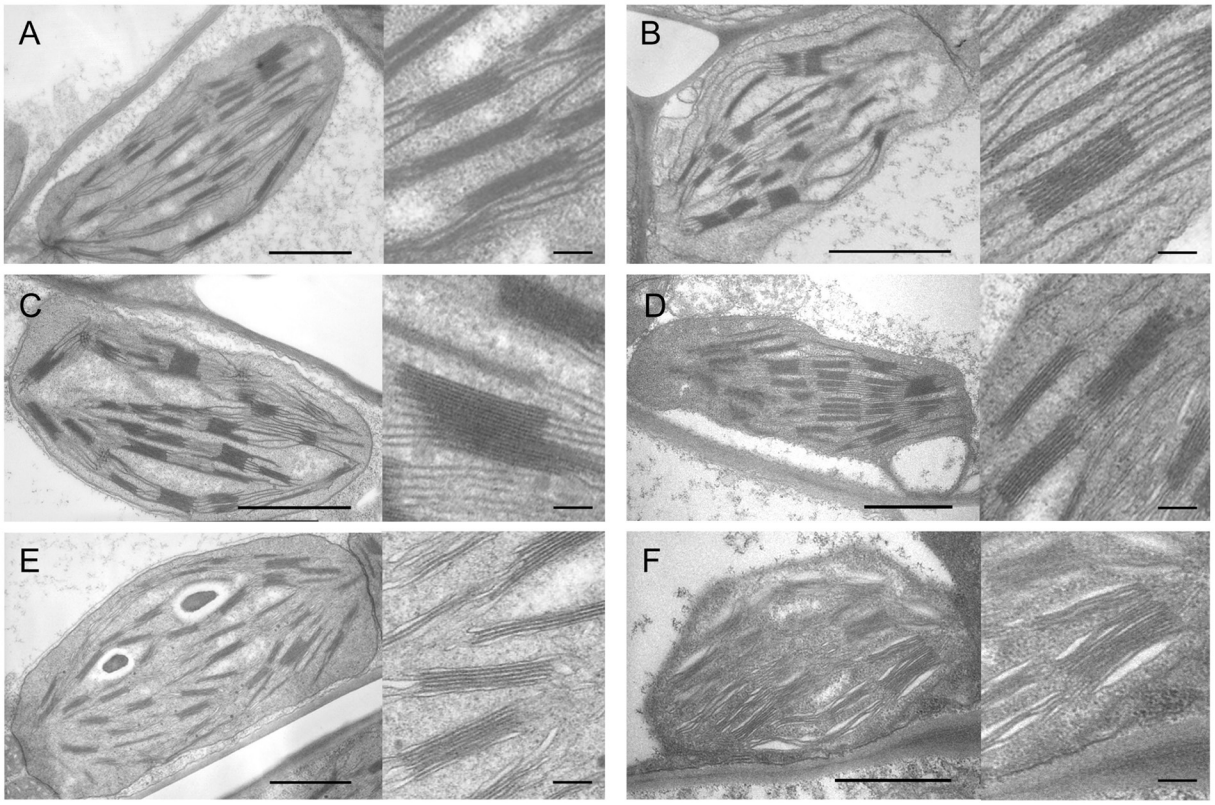

Fig. 10. TEM images of chloroplast ultrastructure of leaflets (A, C, E) and stipules (B, D, F) in *Pisum sativum*. Representative details of grana stacks are shown on the right side of each panel.
(A) Dark-acclimated leaflets; note the well-ordered thylakoid system with several small grana and thylakoids with narrow lumen. (B) Dark-acclimated stipules; the thylakoid system is quite loosely organized and immersed in clear stroma, thylakoid lumen is wider than in (A). (C) Far-red treated leaflets; grana are thicker than under growth light and thylakoid lumen is hardly visible. (D) Far-red treated stipules; the thylakoid organization is essentially similar to (B). (E) Leaflets at the steady-state growth light show starch granules and thylakoids with a larger lumen. (F) Stipules at the steady-state growth light do not show significant accumulation of starch, while the thylakoid system is less ordered than in (E). Bars: 1 μm for the entire chloroplasts, 0.1 μm for details.

Table 2
Granum thickness, single thylakoid thickness and number of thylakoids per granum in leaflets (L) and stipules (S) of *P. sativum* prepared for TEM analyses at the end of the daily dark phase (D), after 15 min far-red treatment (FR) and during growth light at the steady-state (GL). Values are replicates ± standard deviation of *N* determinations from different micrographs belonging to the same type of sample. For statistical comparison of data, one-factor ANOVA test followed by *post hoc* Tuckey's test was used. Differences were not significant ($P \geq 0.05$) for groups with the same letter.

Sample	Granum thickness (μm)	Thylakoid thickness (μm)	Number of thylakoids per granum	*N*
L_D	0.068 ± 0.023^{a}	0.009 ± 0.002^{a}	7.51 ± 2.60^{a}	38
L_{FR}	0.105 ± 0.044^{b}	0.009 ± 0.002^{a}	11.17 ± 4.72^{b}	32
L_{GL}	0.100 ± 0.029^{b}	0.013 ± 0.002^{b}	7.69 ± 2.23^{a}	32
S_D	0.097 ± 0.040^{b}	0.014 ± 0.006^{b}	7.19 ± 2.90^{a}	54
S_{FR}	0.102 ± 0.041^{ab}	0.015 ± 0.004^{b}	8.05 ± 4.79^{a}	26
S_{GL}	0.089 ± 0.030^{ab}	0.014 ± 0.005^{b}	7.85 ± 4.05^{a}	39

Transparency document

The Transparency document associated with this article can be found, in online version.

Acknowledgements

This work was supported by the Italian Ministry of Education, University and Research - “Futuro in Ricerca 2013” program [grant number RBFR1334SB] and the University of Ferrara (FAR2016, FAR2017).

Author contributions

LP, conception and design of the study; MG, CP, PA, CB, acquisition of data; MG, LP, LF, SP, CP, analysis and interpretation of data; MG and LF, drafting the article; SP, critical revision of the article for important intellectual content; all Authors, approval of the final version to be submitted.

References

[1] L.W. Bielczynski, G. Schansker, R. Croce, Effect of light acclimation on the organization of photosystem II super-and sub-complexes in *Arabidopsis thaliana*, Front. Plant Sci. 7 (105) (2016) 1–12.
[2] J. Barber, Photosystem II: the engine of life, Q. Rev. Biophys. 36 (2003) 71–89.
[3] J. Minagawa, Y. Takahashi, Structure, function and assembly of photosystem II and its light-harvesting proteins, Photosynth. Res. 82 (3) (2004) 241–263.
[4] R. Danielsson, M. Suorsa, V. Paakkarinen, P. Albertsson, S. Styring, E. Aro, F. Mamedov, Dimeric and monomeric organization of photosystem II. Distribution of five distinct complexes in the different domains of the thylakoid membrane, J. Biol. Chem. 281 (2006) 14241–14249.
[5] J.P. Dekker, E.J. Boekema, Supramolecular organization of thylakoid membrane proteins in green plants, Biochim. Biophys. Acta (BBA)-Bioenerg. 1706 (1) (2005) 12–39.
[6] S. Caffarri, R. Kouřil, S. Kereïche, E.G. Boekema, R. Croce, Functional architecture of higher plant photosystem II supercomplexes, EMBO J. 28 (19) (2009) 3052–3063.
[7] R. Croce, H. van Amerongen, Light-harvesting and structural organization of photosystem II: from individual complexes to thylakoid membrane, J. Photochem. Photobiol. B Biol. 104 (1) (2011) 142–153.
[8] R. Kouřil, E. Wientjes, J.B. Bultema, R. Croce, E.J. Boekema, High-light vs. low-

light: effect of light acclimation on photosystem II composition and organization in *Arabidopsis thaliana*, Biochim. Biophys. Acta (BBA)-Bioenerg. 1827 (3) (2013) 411–419.
[9] L.S. van Bezouwen, S. Caffarri, R.S. Kale, R. Kouřil, A.W.H. Thunnissen, G.T. Oostergetel, E.J. Boekema, Subunit and chlorophyll organization of the plant photosystem II supercomplex, Nat. Plants 3 (2017) 17080.
[10] X. Wei, X. Su, P. Cao, X. Liu, W. Chang, M. Li, X. Zhang, Z. Liu, Structure of spinach photosystem II-LHCII supercomplex at 3.2 Å resolution, Nature 534 (2016) 69–74.
[11] X. Su, J. Ma, X. Wei, P. Cao, D. Shu, W. Chang, Z. Liu, X. Zhang, M. Li, Structure and assembly mechanism of plant $C_2S_2M_2$-type PSII-LHCII supercomplex, Science 357 (2017) 815–820.
[12] P. Albanese, J. Nield, J.A. Tabares, A. Chiodoni, M. Manfredi, F. Gosetti, E. Marengo, G. Saracco, J. Barber, C. Pagliano, Isolation of novel PSII-LHCII megacomplexes from pea plants characterized by a combination of proteomics and electron microscopy, Photosynth. Res. 130 (1–3) (2016) 19–31.
[13] L. Nosek, D. Semchonok, E.J. Boekema, P. Ilik, R. Kouřil, Structural variability of plant photosystem II megacomplexes in thylakoid membranes, Plant J. 89 (2017) 104–111.
[14] B. Andersson, J.M. Anderson, Lateral heterogeneity in the distribution of chlorophyll-protein complexes of the thylakoid membranes of spinach, Biochim. Biophys. Acta 593 (1980) 427–440.
[15] H. Kirchhoff, S. Haferkamp, J.F. Allen, D.B. Epstein, C.W. Mullineaux, Protein diffusion and macromolecular crowding in thylakoid membranes, Plant Physiol. 146 (4) (2008) 1571–1578.
[16] H. Kirchhoff, M. Li, S. Puthiyaveetil, Sublocalization of cytochrome b_6f complexes in photosynthetic membranes, Trends Plant Sci. 22 (2017) 574–582.
[17] P. Albanese, M. Manfredi, A. Meneghesso, E. Marengo, G. Saracco, J. Barber, T. Morosinotto, C. Pagliano, Dynamic reorganization of photosystem II supercomplexes in response to variations in light intensities, Biochim. Biophys. Acta (BBA)-Bioenerg. 1857 (10) (2016) 1651–1660.
[18] E.L. Apostolova, A.G. Dobrikova, P.I. Ivanova, I.B. Petkanchin, S.G. Taneva, Relationship between the organization of the PSII supercomplex and the functions of the photosynthetic apparatus, J. Photochem. Photobiol. B Biol. 83 (2) (2006) 114–122.
[19] L. Dietzel, K. Bräutigam, T. Pfannschmidt, Photosynthetic acclimation: state transitions and adjustment of photosystem stoichiometry–functional relationships between short-term and long-term light quality acclimation in plants, FEBS J. 275 (6) (2008) 1080–1088.
[20] J.M. Anderson, P. Horton, E.H. Kim, W.S. Chow, Towards elucidation of dynamic structural changes of plant thylakoid architecture, Philos. Trans. R. Soc. Lond. B: Biol. Sci. 367 (1608) (2012) 3515–3524.
[21] T. Schumann, S. Paul, M. Melzer, P. Dörmann, P. Jahns, Plant growth under natural light conditions provides highly flexible short-term acclimation properties toward high light stress, Front. Plant Sci. 8 (2017) 681.
[22] E. Wientjes, H. van Amerongen, R. Croce, LHCII is an antenna of both photosystems after long-term acclimation, Biochim. Biophys. Acta (BBA)-Bioenerg. 1827 (3) (2013) 420–426.
[23] E. Wientjes, H. van Amerongen, R. Croce, Quantum yield of charge separation in photosystem II: functional effect of changes in the antenna size upon light acclimation, J. Phys. Chem. B 117 (38) (2013) 11200–11208.
[24] E. Wientjes, B. Drop, R. Kouřil, E.J. Boekema, R. Croce, During state 1 to state 2 transition in *Arabidopsis thaliana*, the photosystem II supercomplex gets phosphorylated but does not disassemble, J. Biol. Chem. 288 (46) (2013) 32821–32826.
[25] M.A. Schöttler, S.Z. Toth, Photosynthetic complex stoichiometry dynamics in higher plants: environmental acclimation and photosynthetic flux control, Front. Plant Sci. 5 (2014) 188.
[26] L. Pantaleoni, L. Ferroni, C. Baldisserotto, E.M. Aro, S. Pancaldi, Photosystem II organisation in chloroplasts of *Arum italicum* leaf depends on tissue location, Planta 230 (5) (2009) 1019–1031.
[27] J.M. Anderson, W.S. Chow, D.J. Goodchild, Thylakoid membrane organisation in sun/shade acclimation, Funct. Plant Biol. 15 (2) (1988) 11–26.
[28] H. Kirchhoff, Structure-function relationships in photosynthetic membranes: challenges and emerging fields, Plant Sci. 266 (2018) 76–82.
[29] J. Minagawa, Dynamic reorganization of photosynthetic supercomplexes during environmental acclimation of photosynthesis, Front. Plant Sci. 4 (2013) 513.
[30] B. Demmig-Adams, C.M. Cohu, O. Muller, W.W. Adams III, Modulation of photosynthetic energy conversion efficiency in nature: from seconds to seasons, Photosynth. Res. 113 (2012) 75–88.
[31] P. Jahns, A.R. Holzwarth, The role of the xanthophyll cycle and of lutein in photoprotection of photosystem II, Biochim. Biophys. Acta (BBA)-Bioenerg. 1817 (2012) 182–193.
[32] S. Matsubara, B. Förster, M. Waterman, S.A. Robinson, B.J. Pogson, B. Gunning, B. Osmond, From ecophysiology to phenomics: some implications of photoprotection and shade–sun acclimation in situ for dynamics of thylakoids in vitro, Philos. Trans. R. Soc. B 367 (2012) 3503–3514.
[33] A.V. Ruban, M.P. Johnson, C.D. Duffy, The photoprotective molecular switch in the photosystem II antenna, Biochim. Biophys. Acta (BBA)-Bioenerg. 1817 (1) (2012) 167–181.
[34] M. Goldschmidt-Clermont, R. Bassi, Sharing light between two photosystems: mechanism of state transitions, Curr. Opin. Plant Biol. 25 (2015) 71–78.
[35] J.F. Allen, J. Bennett, K.E. Steinback, C.J. Arntzen, Chloroplast protein phosphorylation couples plastoquinone redox state to distribution of excitation energy between photosystems, Nature 291 (5810) (1981) 25–29.
[36] P. Pesaresi, A. Hertle, M. Pribil, T. Kleine, R. Wagner, H. Strissel, A. Ihnatowicz, V. Bonardi, M. Scharfenberg, A. Schneider, T. Pfannschmidt, *Arabidopsis* STN7 kinase provides a link between short-and long-term photosynthetic acclimation, Plant Cell 21 (8) (2009) 2402–2423.
[37] L. Dietzel, K. Bräutigam, S. Steiner, K. Schüffler, B. Lepetit, B. Grimm, M.A. Schöttler, T. Pfannschmidt, Photosystem II supercomplex remodeling serves as an entry mechanism for state transitions in *Arabidopsis*, Plant Cell 23 (8) (2011) 2964–2977.
[38] R. Kouřil, A. Zygadlo, A.A. Arteni, C.D. de Wit, J.P. Dekker, P.E. Jensen, H.V. Schellen, E.J. Boekema, Structural characterization of a complex of photosystem I and light-harvesting complex II of *Arabidopsis thaliana*, Biochemistry 44 (33) (2005) 10935–10940.
[39] P. Galka, S. Santabarbara, T.T.H. Khuong, H. Degand, P. Morsomme, R.C. Jennings, E.J. Boekema, S. Caffarri, Functional analyses of the plant photosystem I–light-harvesting complex II supercomplex reveal that light-harvesting complex II loosely bound to photosystem II is a very efficient antenna for photosystem I in state II, Plant Cell 24 (7) (2012) 2963–2978.
[40] M. Suorsa, M. Rantala, F. Mamedov, M. Lespinasse, A. Trotta, M. Grieco, E. Vuorio, M. Tikkanen, S. Järvi, E.M. Aro, Light acclimation involves dynamic re-organization of the pigment–protein megacomplexes in non-appressed thylakoid domains, Plant J. 84 (2) (2015) 360–373.
[41] M. Grieco, M. Suorsa, A. Jajoo, M. Tikkanen, E.M. Aro, Light-harvesting II antenna trimers connect energetically the entire photosynthetic machinery—including both photosystems II and I, Biochim. Biophys. Acta (BBA)-Bioenerg. 1847 (6) (2015) 607–619.
[42] M. Tikkanen, M. Piippo, M. Suorsa, S. Sirpiö, P. Mulo, J. Vainonen, A.V. Vener, Y. Allahverdiyeva, E.M. Aro, State transitions revised – a buffering system for dynamic low light acclimation of *Arabidopsis*, Plant Mol. Biol. 62 (2006) 779–793.
[43] M. Tikkanen, E.M. Aro, Thylakoid protein phosphorylation in dynamic regulation of photosystem II in higher plants, Biochim. Biophys. Acta (BBA)-Bioenerg. 1817 (1) (2012) 232–238.
[44] M. Yokono, S. Akimoto, Energy transfer and distribution in photosystem super/megacomplexes of plants, Curr. Opin. Biotechnol. 54 (2018) 54–56.
[45] P. Albanese, R. Melero, B.D. Engel, A. Grinzato, P. Berto, M. Manfredi, A. Chiodoni, J. Vargas, C.O. Sanchez Sorzano, E. Marengo, G. Saracco, G. Zanotti, J.-M. Carazo, C. Pagliano, Pea PSII-LHCII supercomplexes form pairs by making connections across the stromal gap, Sci. Rep. 7 (2017) 10067.
[46] C. Pagliano, S. Barera, F. Chimirri, G. Saracco, J. Barber, Comparison of the α and β isomeric forms of the detergent n-dodecyl-D-maltoside for solubilizing photosynthetic complexes from pea thylakoid membranes, Biochim. Biophys. Acta (BBA)-Bioenerg. 1817 (8) (2012) 1506–1515.
[47] C. Pagliano, J. Nield, F. Marsano, T. Pape, S. Barera, G. Saracco, J. Barber, Proteomic characterization and three-dimensional electron microscopy study of PSII–LHCII supercomplexes from higher plants, Biochim. Biophys. Acta (BBA)-Bioenerg. 1837 (9) (2014) 1454–1462.
[48] I. Rumak, R. Mazur, K. Gieczewska, J. Kozioł-Lipińska, B. Kierdaszuk, W.P. Michalski, B.J. Shiell, J.H. Venema, W.J. Vredenberg, A. Mostowska, M. Garstka, Correlation between spatial (3D) structure of pea and bean thylakoid membranes and arrangement of chlorophyll-protein complexes, BMC Plant Biol. 12 (2012) 72.
[49] D.E. Collier, B. Grodzinski, Growth and maintenance respiration of leaflet, stipule, tendril, rachis, and petiole tissues that make up the compound leaf of pea (*Pisum sativum*), Can. J. Bot. 74 (8) (1996) 1331–1337.
[50] R. Côté, B. Grodzinski, Photosynthesis, photorespiration and partitioning in leaflets, stipules and tendrils of *Pisum sativum*, Current Research in Photosynthesis, Springer, Netherlands, 1990, pp. 2873–2876.
[51] R. Côté, J.M. Gerrath, C.A. Peterson, B. Grodzinski, Sink to source transition in tendrils of a semileafless mutant, *Pisum sativum* cv Curly, Plant Physiol. 100 (4) (1992) 1640–1648.
[52] V. Sharma, A.K. Sinha, S. Chaudhary, A. Priyadarshini, B.N. Tripathi, S. Kumar, Genetic analysis of structure and function of stipules in pea *Pisum sativum*, Proc. Indian Natl. Sci. Acad. 78 (2012) 9–34.
[53] A.R. Wellburn, The spectral determination of chlorophyll *a* and chlorophyll *b*, as well as total carotenoids, using various solvents with spectrophotometers of different resolution, J. Plant Physiol. 114 (1994) 307–313.
[54] M.S. Peek, E. Russek-Cohen, A.D. Wait, I.N. Forseth, Physiological response curve analysis using nonlinear mixed models, Oecologia 132 (2) (2002) 175–180.
[55] L. Hendrickson, R.T. Furbank, W.S. Chow, A simple alternative approach to assessing the fate of absorbed light energy using chlorophyll fluorescence, Photosynth. Res. 82 (2004) 73–81.
[56] D. Lazàr, Parameters of photosynthetic energy partitioning, J. Plant Physiol. 175 (2015) 131–147.
[57] H.M. Kalaji, G. Schansker, M. Brestic, F. Bussotti, A. Calatayud, L. Ferroni, V. Goltsev, L. Guidi, A. Jajoo, P. Li, P. Losciale, V.K. Mishra, A.N. Misra, S.G. Nebauer, S. Pancaldi, C. Penella, M. Pollastrini, K. Suresh, E. Tambussi, M. Yanniccari, M. Zivcak, M.G. Cetner, I.A. Samborska, A. Stirbet, K. Olsovska, K. Kunderlikova, H. Shelonzek, A. Rusinowski, W. Baba, Frequently asked questions about chlorophyll fluorescence, the sequel, Photosynth. Res. 132 (2017) 13–66.
[58] M. Tikkanen, S. Rantala, E.M. Aro, Electron flow from PSII to PSI under high light is controlled by PGR5 but not by PSBS, Front. Plant Sci. 6 (2015) 521.
[59] M. Tikkanen, S. Rantala, M. Grieco, E.M. Aro, Comparative analysis of mutant plants impaired in the main regulatory mechanisms of photosynthetic light reactions – from biophysical measurements to molecular mechanisms, Plant Physiol. Biochem. 112 (2017) 290–301.
[60] H. Lokstein, H. Härtel, P. Hoffmann, P. Woitke, G. Renger, The role of light-harvesting complex II in excess energy dissipation: an in-vivo fluorescence study on the origin of high-energy quenching, J. Photochem. Photobiol. 26 (1994) 175–184.
[61] L. Ferroni, M. Angeleri, P. Pantaleoni, C. Pagliano, P. Longoni, F. Marsano, E.M. Aro, M. Suorsa, C. Baldisserotto, M. Giovanardi, R. Cella, S. Pancaldi, Light-

dependent reversible phosphorylation of the minor photosystem II antenna Lhcb6 (CP24) occurs in lycophytes, Plant J. 77 (2014) 893–905.
[62] S. Järvi, M. Suorsa, V. Paakkarinen, E.M. Aro, Optimized native gel systems for separation of thylakoid protein complexes: novel super- and megacomplexes, Biochem. J. 439 (2011) 207–214.
[63] U.K. Laemmli, Cleavage of structural proteins during the assembly of the head of bacteriophage T4, Nature 227 (5259) (1970) 680–685.
[64] L. Ferroni, M. Suorsa, E.M. Aro, C. Baldisserotto, S. Pancaldi, Light acclimation in the lycophyte *Selaginella martensii* depends on changes in the amount of photosystems and on the flexibility of the light-harvesting complex II antenna association with both photosystems, New Phytol. 211 (2) (2016) 554–568.
[65] C. Baldisserotto, L. Ferroni, E. Anfuso, A. Pagnoni, M.P. Fasulo, S. Pancaldi, Responses of *Trapa natans* L. floating laminae to high concentrations of manganese, Protoplasma 231 (1) (2007) 65–82.
[66] R.J. Ritchie, Consistent sets of spectrophotometric chlorophyll equations for acetone, methanol and ethanol solvents, Photosynth. Res. 89 (2006) 27–41.
[67] H. Lichtenthaler, F. Babani, M. Navrátil, K. Buschmann, Chlorophyll fluorescence kinetics, photosynthetic activity, and pigment composition of blue-shade and half-shade leaves as compared to sun and shade leaves of different trees, Photosynth. Res. 117 (2013) 355–366.
[68] M. Grieco, M. Tikkanen, V. Paakkarinen, S. Kangasjärvi, E.M. Aro, Steady state phosphorylation of light-harvesting complex II proteins preserves photosystem I under fluctuating white light, Plant Physiol. 160 (2012) 1896–1910.
[69] E.M. Aro, M. Suorsa, A. Rokka, Y. Allahverdiyeva, V. Paakkarinen, A. Saleem, N. Battchikova, E. Rintamäki, Dynamics of photosystem II: a proteomic approach to thylakoid protein complexes, J. Exp. Bot. 56 (411) (2005) 347–356.
[70] M. Pietrzykowska, M. Suorsa, D.A. Semchonok, M. Tikkanen, E.J. Boekema, E.M. Aro, S. Jansson, The light-harvesting chlorophyll a/b binding proteins Lhcb1 and Lhcb2 play complementary roles during state transitions in *Arabidopsis*, Plant Cell 26 (9) (2014) 3646–3660.
[71] P. Longoni, D. Douchi, F. Cariti, G. Fucile, M. Goldschmidt-Clermont, Phosphorylation of the light-harvesting complex II isoform Lhcb2 is central to state transitions, Plant Physiol. 169 (2015) 2874–2883.
[72] M. Rantala, M. Tikkanen, E.M. Aro, Proteomic characterization of hierarchical megacomplex formation in *Arabidopsis* thylakoid membrane, Plant J. 92 (2017) 951–962.
[73] P.R. Rozak, R.M. Seiser, W.F. Wacholtz, R.R. Wise, Rapid, reversible alterations in spinach thylakoid appression upon changes in light intensity, Plant Cell Environ. 25 (3) (2002) 421–429.
[74] J. Flexas, A. Diaz-Espejo, M.A. Conesa, R.E. Coopman, C. Douthe, J. Gago, A. Gallé, J. Galmez, H. Medrano, M. Ribas-Carbo, M. Tomàs, U. Niinemets, Mesophyll conductance to CO_2 and Rubisco as targets for improving intrinsic water use efficiency in C3 plants, Plant Cell Environ. 39 (2016) 965–982.
[75] B. Demmig-Adams, J.J. Stewart, W.W. Adams III, Environmental regulation of intrinsic photosynthetic capacity: an integrated view, Curr. Opin. Plant Biol. 37 (2017) 34–41.
[76] C. Klughammer, U. Schreiber, Complementary PS II quantum yields calculated from simple fluorescence parameters measured by PAM fluorometry and the saturation pulse method, PAM Appl. Notes 1 (2) (2008).
[77] Y. Munekage, M. Hojo, J. Meurer, T. Endo, M. Tasaka, T. Shikanai, PGR5 is involved in cyclic electron flow around photosystem I and is essential for photoprotection in *Arabidopsis*, Cell 110 (2002) 361–371.
[78] M. Suorsa, S. Järvi, M. Grieco, M. Nurmi, M. Pietrzykowska, M. Rantala, S. Kangasjärvi, V. Paakkarinen, M. Tikkanen, S. Jansson, E.M. Aro, PROTON GRADIENT REGULATION5 is essential for proper acclimation of *Arabidopsis* photosystem I to naturally and artificially fluctuating light conditions, Plant Cell 24 (7) (2012) 2934–2948.
[79] J.D. Rochaix, Regulation of photosynthetic electron transport, Biochim. Biophys. Acta (BBA)-Bioenerg. 1807 (2011) 375–383.
[80] S. Bellafiore, F. Barneche, G. Peltier, J.D. Rochaix, State transitions and light adaptation require chloroplast thylakoid protein kinase STN7, Nature 433 (7028) (2005) 892–895.
[81] M. Iwai, M. Yokono, A. Nakano, Visualizing structural dynamics of thylakoid membranes, Sci. Rep. 4 (2014).
[82] T. Shikanai, H. Yamamoto, Contribution of cyclic and pseudo-cyclic electron transport to the formation of proton motive force in chloroplasts, Mol. Plant 10 (2017) 20–29.
[83] T. Tongra, S. Bharti, A. Jajoo, Cyclic electron flow around photosystem I is enhanced at low pH, Plant Physiol. Biochem. 83 (2014) 194–199.
[84] M. Yokono, A. Takabayashi, S. Akimoto, A. Tanaka, A megacomplex composed of both photosystem reaction centres in higher plants, Nat. Commun. 6 (2015) 6675.
[85] L. Ferroni, S. Cucuzza, M. Angeleri, E.M. Aro, C. Pagliano, M. Giovanardi, C. Baldisserotto, S. Pancaldi, In the lycophyte *Selaginella martensii* is the “extra-qT” related to energy spillover? Insights into photoprotection in ancestral vascular plants, Environ. Exp. Bot. (2018), http://dx.doi.org/10.1016/j.envexpbot.2017.10.023.
[86] M. Tikkanen, M. Grieco, S. Kangasjärvi, E.M. Aro, Thylakoid protein phosphorylation in higher plant chloroplasts optimizes electron transfer under fluctuating light, Plant Physiol. 152 (2) (2010) 723–735.
[87] M. Pribil, M. Labs, D. Leister, Structure and dynamics of thylakoids in land plants, J. Exp. Bot. 65 (2014) 1955–1972.
[88] P. Pesaresi, Ch. Lunde, P. Jahns, D. Tarantino, J. Meurer, C. Varotto, R.-D. Hirtz, C. Soave, H.V. Scheller, F. Salamini, D. Leister, A stable LHCII-PSI aggregate and suppression of photosynthetic state transition in the psae1-1 mutant of *Arabidopsis thaliana*, Planta 215 (2002) 940–948.
[89] H. Kirchhoff, Structural constraints for protein repair in plant photosynthetic membranes, Plant Signal. Behav. 8 (2013) e23634.